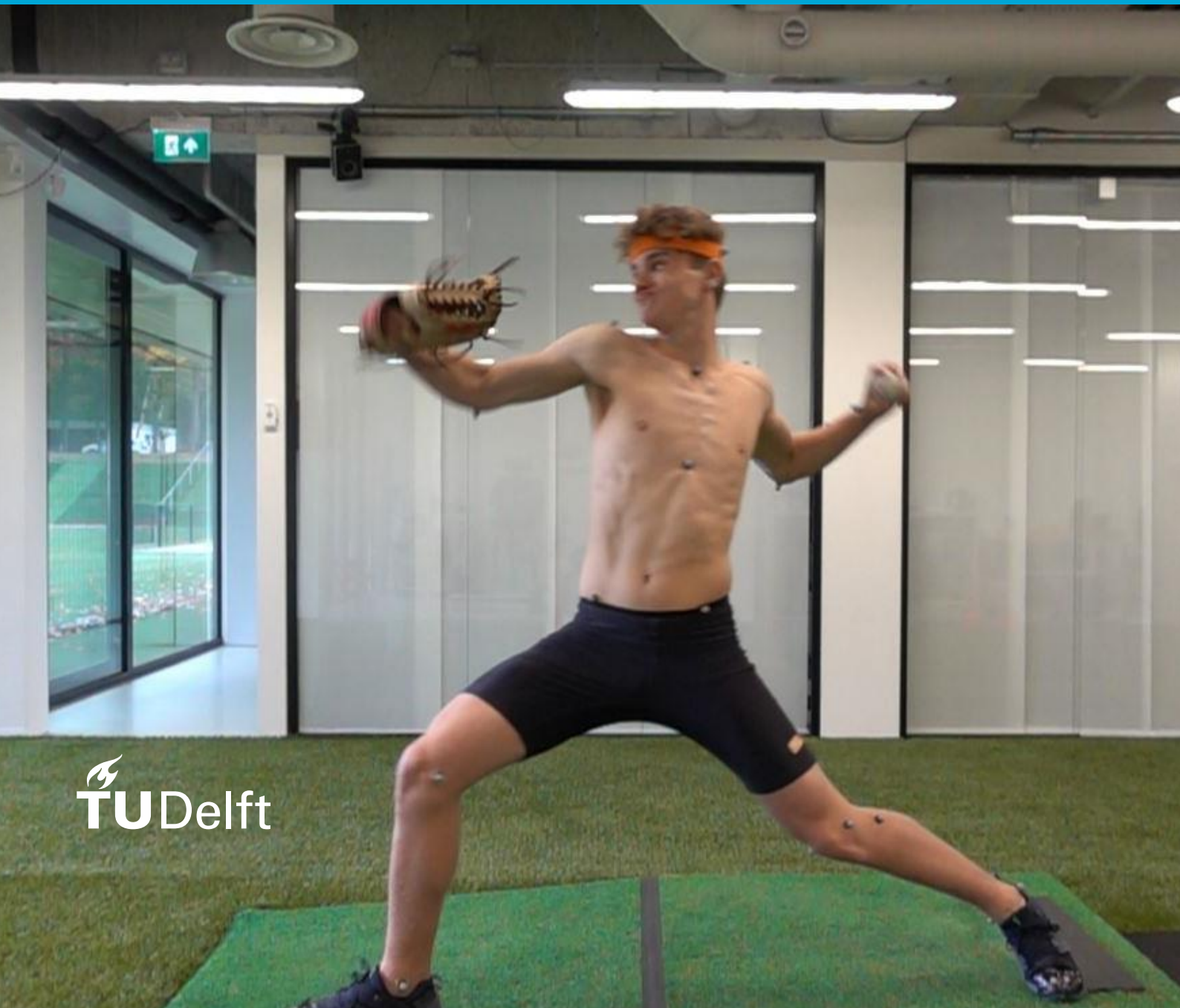# Establishing the elbow load and the within-pitcher load variability during a baseball pitch in relation to the ball speed

F. F. Bouman

Establishing the elbow load and the within-pitcher load variability during a baseball pitch in relation to the ball speed

A Master thesis

by

Foskien Bouman

Student number: 4298764

in partial fulfilment of the requirements for the degree of

Master of Science

in

Biomedical Engineering

at the Delft University of Technology

Daily supervisor: B. van Trigt, PhD candidate
Supervisor: Proj. dr. H.E.J. Veeger
Thesis committee member: Prof. dr. F.C.T. van der Helm

T̃U Delft

Abstract

Ulnar collateral ligament (UCL) injuries are common in baseball pitching. The elbow external valgus torque is assumed to be indicative for the applied load on the UCL.

This study investigated the maximum external valgus and extension torque and their corresponding load variability during a baseball pitch and the relationship between the magnitude and the within-pitcher load variability of these elbow torques. Furthermore, this study investigated to what extend the elbow torques and the ball speed are related. Eleven Dutch AAA pitchers each threw 25 fastballs. The motion was captured with an optical motion capture system. The ball speed was measured with a radar gun. The data of the upper body, in particular the elbow torques, were analysed using a custom-made 3D inverse dynamics model. The results show that the within-pitcher load variability differs among pitchers. A higher applied elbow torque compared to other pitchers indicates a higher within-pitcher variability. From these results, both a higher valgus torque and a higher within-pitcher load variability are expected to lead to higher injury risk. It is advised not to take one pitch per pitcher into account since it cannot represent all the pitches, especially if only the fastest is selected. Among the pitchers, ball speed is found not to be a good indicator for the elbow torques. Within a pitcher, the ball speed serves better as an indicator. This study emphasises the importance of analysing each pitcher's results individually instead of comparing them to the whole group.

Introduction

In 2017, 15.64 million people played baseball in the US, making it the second most popular sport in the US and the seventh on the world's ranking (Gough, 2018; Sports show, 2020). According to a study of Dillmann et al. (1993), baseball pitching is one of the fastest recorded human movements (Dillman et al., 1993). This fast movement demands a lot from the human body and makes it prone to injuries. Comparing positions among baseball players, pitchers cover 49% to 55% of the placings on the baseball disabled list (Conte et al., 2001; Posner et al., 2011). A common injury among pitchers is a strain or rupture of the ulnar collateral ligament (UCL). In 2019, 29.8% of all pitchers in the MLB (highest baseball division in the USA) had undergone a UCL reconstruction surgery (Roegele, 2018). Comparing elbow surgeries between 1995 and 1999 (total of 184 surgeries) with surgeries performed between 2000 and 2004 (total of 624 surgeries), six times more elbow surgeries are executed on high school pitchers (Fleisig et al., 2006). It is difficult to separate which part of this increase is on account of more injuries or on the better recognition of injuries over time or on the increase of high school baseball pitchers. Nevertheless, it is clear that injuries are common and should be prevented in any way possible.

A baseball pitch can be described according to characteristic events that occur during the motion; *foot contact* (FC), the moment the stride foot touches the ground, *maximum external rotation* (MER), which is the moment the humerus is in maximal external rotation with respect to the thorax, and *ball release* (BR) which is the moment the ball leaves the hand. The time between *foot contact* and *ball release* is approximately 140 milliseconds (Fleisig et al., 1995). During the pitching motion between *foot contact* and *ball release*, an external torque is applied around the elbow, which can be divided into two major components. The first component is the external extension torque which is held responsible for the elbow movement during the baseball pitch. The second component is the external valgus torque, which must be withstood to maintain elbow stability during the pitch.

During the fast performed baseball pitch, a high external valgus torque is applied around the elbow, which is counteracted by an internal varus torque, with the help of both functional stabilisers and structural stabilisers. The elbow muscles are assumed to serve as functional stabilisers, which deliver a counteracting internal varus torque (Lin et al., 2007; van Trigt et al., 2021). The structural stabilisers are the elbow's geometry and the ligaments that provides stability when an external valgus torque is applied, like the UCL (van Trigt et al., 2021). Previous research found that high school pitchers' peak external valgus torque, performing a fastball, is around 50 Nm (Fleisig et al., 1999; Gasparutto et al., 2016; Okoroha et al., 2018). The peak valgus torque occurs around *MER* (Buffi et al., 2015; Fleisig et al., 1995). An increased valgus torque around the elbow is considered to be a risk indicator for a UCL injury (Aguinaldo & Chambers, 2009; Sabick et al., 2004; Wilk et al., 2014). A study by Hurd, Kaufman & Murphy (2011), who studied the behaviour of the UCL, using an MRI evaluation, found that after applying a high peak valgus torque, the UCL showed an abnormal appearance, expressed as a thickening of the UCL (Hurd et al., 2011). Due to the structural stability task of the UCL and the expected relationship between peak valgus torque and a UCL injury, it is reasonable to assume that the valgus torque can be used as a proxy for the applied UCL load.

In biomechanical models, the elbow is considered to act as a hinge joint, where only flexion and extension motion is possible (van Trigt et al., 2021; Wu et al., 2005). The amount of elbow extension, related to the external extension torque, influence the execution of the baseball pitch between *foot contact* and *ball release*. Previous research on high school pitchers found that the peak extension torque is approximately 40 Nm (Fleisig et al., 1999; Gasparutto et al., 2016). The peak extension torque occurs just before *ball release*, shortly after the peak valgus torque (Fleisig et al., 1995;

Gasparutto et al., 2016). A study by Stodden et al. (2005) found that a higher peak extension torque around the elbow is related to a higher ball velocity (Stodden et al., 2005). To gain more insight into the baseball pitch's performance, the analysis of the external extension torque is essential.

The maximum ball speed is often used as a performance measure in baseball pitching (Stodden et al., 2005). A commonly used pitch type is the fastball. Performing a fastball leads to the highest ball speed compared to other pitch types, like the curveball, change-up and slider (Adler, 2019; Brooks, 2020). Previous research shows that high school pitchers throw fastballs at approximately 76 mph (where the MLB pitchers often approach 100 mph) (Anz et al., 2010; Fleisig et al., 1999; Okoroha et al., 2018). Ball speed also suits well as a proxy for performance since it is one of the few accessible, quantifiable, and external parameters during a baseball pitch. However, throwing as fast as possible also comes with a downside since an increased ball speed is obviously related to an increased risk for an elbow injury. Bushnell et al. (2010) noticed that from their 25 professional pitchers, those who pitched with the highest velocity were also those who required a UCL surgery (Bushnell et al., 2010). In the study of Okoroha et al. (2018), the fastball caused the highest arm velocities and the highest elbow torques in comparison to other pitch types (which have a lower ball speed) (Okoroha et al., 2018). A pitcher should strive for optimal pitching efficiency, which means that he maximises the output (a high ball speed) but minimises the injury risks (by not applying an excessive load on the elbow, which means not applying an excessive valgus torque) (Aguinaldo & Chambers, 2009).

There is no doubt that participants differ from each other and that their kinetics will also differ. This between-pitcher variability is represented as the standard deviation of the whole group and is valuable when comparing the performance or risk factors among certain groups based on for example age, competence, or injury history (Aguinaldo & Chambers, 2009; Fleisig et al., 1995). For each pitcher individually, researchers often select only one or a few pitches, often by ball speed, for their analysis, even if multiple pitches are thrown. Based on these few pitches, they conclude that the differences among the pitches are minor (Aguinaldo & Chambers, 2009; Fleisig et al., 1995). Alternatively, they invoke older researches that state that all the pitches of a pitcher can be considered consistent (Feltner & Dapena, 1986; Pappas et al., 1985). The question arises whether this is a valid approach as more and more researches found that within-pitcher variability can provide insight into a pitcher's behaviour (Bartlett et al., 2007; Davids et al., 2003; Scarborough et al., 2018; Stodden et al., 2001; van Trigt et al., 2020). Another use of within-pitcher variability is found in the research of van Trigt et al. (2020), who introduced a model that relates the risk for an injury with the within-pitcher load variability (variance of the kinetic parameters) and the load capacity of a pitcher. They expect that a higher within-pitcher load variability will increase the risk for an injury (van Trigt et al., 2020). Even though this expectation and the knowledge within-pitcher load variability could provide on performance improvements or risk indicators of a particular pitcher, research on within-pitcher load variability has to our knowledge never been executed. This emphasises the importance of performing this type of research.

Altogether, the first objective of this study is to examine the maximum elbow torques and their variability, both within- and between-pitchers, of a baseball pitch in a group of Dutch AAA pitchers. The second objective is to investigate if the magnitude and the within-pitcher variability of the maximum elbow torques among pitchers are related. The third objective is to investigate if a relationship is present between the maximum elbow torques and the ball speed.

Method

Participants

Eleven male Dutch AAA pitchers participated in this study at a mean age of 17.5 ± 2 years. Their mean body mass was 80.6 ± 11.1 kg, and their mean body height was 186.5 ± 5.6 cm. Nine pitchers threw with their right hand, where two pitchers threw with their left hand. All participants were uninjured and free of pain and soreness and experienced no range of motion restrictions. The research was entirely voluntary; the pitcher was allowed to stop the measurements at any moment without consequences. After being informed about the content and the study's purpose, all participants signed written informed consent. The local ethics committee of the Faculty of Behavioural and Movement Sciences approved the study (reference number: VCWE-2019-033).

Procedure

The measurements were performed at the Royal Netherlands Football Association testing facility. The participants were instructed to wear tight-fitting trousers or shorts and indoor shoes solely. Forty-three reflective markers (10mm diameter) were attached with double-sided tape directly on the (with alcohol cleaned) skin at body landmarks all over the body. After the marker set up, the participant was allowed unlimited warming up, consisting of running, throwing and performing some warm-up pitches. The pitcher threw from a pitching mound towards a square strike zone (0.64m x 0.38m) at a regular game distance of 18.44 meter while wearing a glove. When ready, the pitcher was asked to throw 25 fastballs as fast and as accurate as possible, aiming at the strike zone.

Data acquisition

The motion was captured using an eight-camera motion analysis system of Vicon (Vicon Motion Systems Ltd.) with a sample frequency of 400 Hz. All pitches were also recorded with a high-speed camera (sample frequency of 240Hz) to serve afterwards as a tool to check if a marker had fallen off. The ball speed of each pitch was captured with a radar gun (Stalker Pro II Sport) from a position close to the target, pointing in the direction of the pitcher, just before the ball hit the target.

Data analysis

Position data were subtracted from the Vicon system, and all the calculations were performed in Python, version 3.7 (Van Rossum & Drake, 2009). If a marker flew off before *ball release* or if a marker could not correctly be reconstructed, the corresponding pitch was not included. Participant eleven was not allowed, due to pitching restrictions, to throw more than 20 pitches. Additionally, fourteen pitches were excluded due to the above-stated protocol. This left 256 pitches available for analysis of the 275 performed (see Appendix B, Table 1 which pitches were not included).
The analysis was performed using a custom-made 3D inverse dynamics model (for more information, see Appendix A). This model focused solely on the upper body. The raw data were manually pre-processed to correct for switching markers. The pitch event of *foot contact* was determined as the moment that the forward velocity of the toe was smaller than 0.3 m/s. The pitch event of *ball release* was determined as the moment after *foot contact* that the position of the wrist exceeded the position of the elbow in the forward direction. The motion data were then interpolated with a 3rd order cubic spline polynomial, cut at *foot contact* and *ball release*, and filtered with a 4th order

Butterworth filter with a cut-off frequency of 12.5 Hz (see Appendix B, Figures 1 and 2 for a sensitivity test). For each segment (hand, forearm, upperarm, trunk, and pelvis), an anatomical coordinate system was made according to the ISB recommendations (Wu et al., 2005), shown in Figure 1. Combining this anatomical coordinate system with the segment data and with the scaling factors of De Leva et al. (1996) and Zatsiorsky et al. (1990), the kinematics of the segments were calculated (de Leva, 1996; Zatsiorsky, 1990, 2002). With this information and using the Newton-Euler method, the global joint forces (at the distal and proximal joints) and global joint torques (at the proximal joint) of each segment were calculated. With the rotation matrices, the global joint torques were transformed into anatomical joint torques for each segment.

At the analysis of this study, a top-down approach was applied where the anatomical elbow torques were investigated. The model calculated the internal elbow torques, but this study evaluated the equal-sized external valgus and external extension torques. For the elbow torque calculation, the markers at the following bony landmarks on the throwing arm are used: Interphalangealis proximal III (HIP3), head of the ulna (US), styloid processes of the radius (RS), the lateral epicondyle (LHE), and the medial epicondyle (MHE). The maximum valgus and extension torques were determined as the highest values between the instants of *foot contact* and *ball release*. The standard deviations of the maximum valgus and extension torque were calculated over the number of included performed pitches (maximum of 25) of each participant. This standard deviation represented within-pitcher variability. The ball speed's within-pitcher variability was determined as the standard deviation of the ball speed, measured with the radar gun, over the number of included performed pitches of each participant.

Figure 1: Local and global coordinate systems of the upper extremity.

Statistical analysis

The maximum valgus torque and maximum extension torque of each participant were checked for normality using the Shapiro-Wilk test. Two types of statistical tests were performed on the data. If the standard deviation was part of the analysis, only eleven data points were available (one for each participant). A linear regression was then performed on these eleven data points to evaluate the relationship between a specific standard deviation and a magnitude, using the Scipy statistical package (Virtanen et al., 2020). The correlation was calculated using a Pearson correlation method. In case the magnitudes of the elbow torques were compared to the ball speed, or in case the elbow torques' reciprocal magnitudes were compared, 256 data points were available. A panel fixed effect ordinary least squares statistical analysis is applied. The panel analysis means that the calculation considers which pitches belonged to which participant. The fixed effects defines that the panels are based on entities (here: participants) and not on time. To apply this panel statistical analysis, a Linear Model Estimation package, version 4.21, was used (Sheppard, 2021). To consider how much of the dependent parameter's variation is defined by the independent parameter, the r^2 is evaluated in this analysis. To determine statistical significance, the alpha level was set to 0.05. The statistical analysis was performed in Python, version 3.7 (Van Rossum & Drake, 2009).
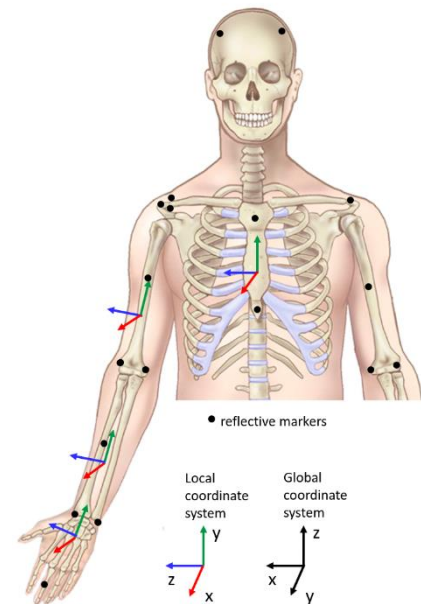
Results

The course of the elbow torques performing a fastball pitch, between *foot contact* and *ball release,* is illustrated in Figure 2. The maximum valgus torque (blue line) occurs first, the maximum extension torque (green line) occurs afterwards just before *ball release*.
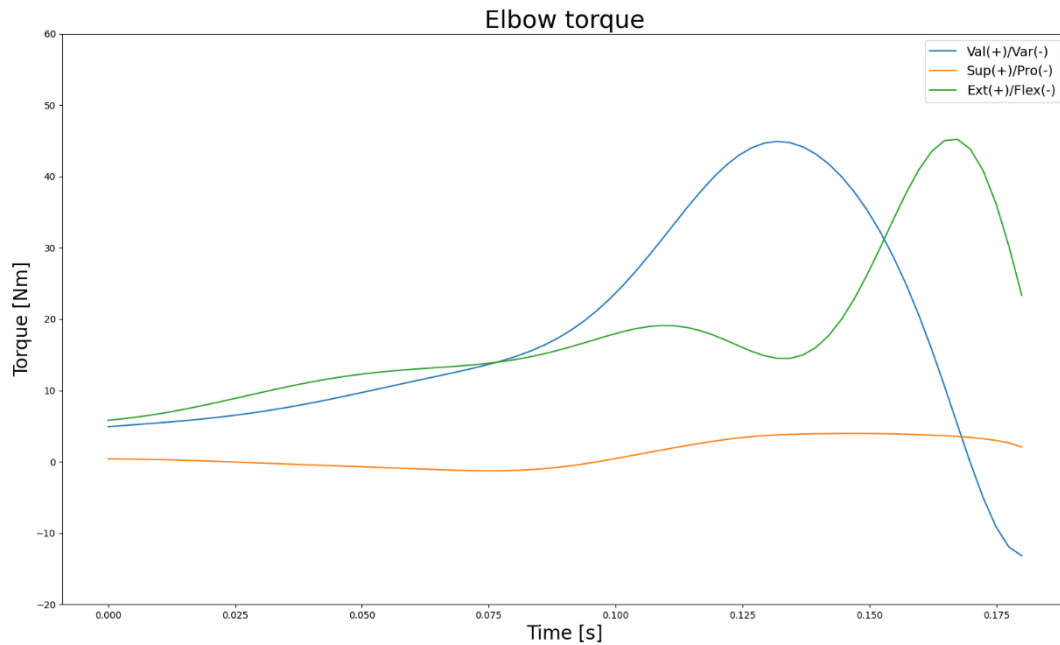

Figure 2: Illustration of the elbow torque between foot contact and ball release (participant 1, pitch 01)

Table 1: Mean and standard deviation (within variability) of the maximum valgus torque, maximum extension torque and ball speed for each participant. The last column represents the number of pitches suited for analysis of each participant (maximum of 25). The last row displays the average values and the standard deviation (between variability) over all participants.

Pitcher	max Valgus torque [Nm]	max Extension torque [Nm]	Ball speed [mph]	Number of pitches included
PP01	42,3 ± 3,68	42,5 ± 2,54	80,7 ± 1,22	24
PP02	39,9 ± 1,67	47,4 ± 1,99	76,1 ± 1,47	25
PP03	25,9 ± 1,79	25,4 ± 1,69	71,9 ± 2,01	25
PP04	32,2 ± 1,08	35,3 ± 1,58	79,5 ± 1,12	24
PP05	33,3 ± 2,08	41,9 ± 1,64	76,4 ± 1,72	25
PP06	45,5 ± 3,46	48,1 ± 2,73	80,9 ± 1,25	20
PP07	36,0 ± 2,10	43,2 ± 1,11	74,5 ± 1,10	23
PP08	47,0 ± 3,33	43,9 ± 2,41	76,7 ± 1,63	24
PP09	37,5 ± 2,79	35,0 ± 3,81	77,0 ± 1,10	23
PP10	52,3 ± 2,68	54,4 ± 2,58	73,1 ± 1,72	24
PP11	39,8 ± 2,81	48,4 ± 3,67	76,0 ± 1,52	19
Average	39,3 ± 7,11	42,4 ± 7,54	76,6 ± 2,75	23

Within-pitcher and between-pitcher load variability

The average and standard deviation of the maximum valgus torque, the maximum extension torque and the ball speed of each participant are shown in Table 1.

The maximum external valgus torque and external extension torque distributions are shown in Figure 3. The distributions differ in the mean maximum valgus/extension torque applied and in the standard deviation per participant (Table 1). The distribution of each participant is checked on normality, see Appendix B Table 1 of which participant the elbow torques were normally distributed. When comparing the elbow kinetics' magnitude with the corresponding within-pitcher variability between the participants, a significant (or near-significant) positive correlation is found (Table 2).
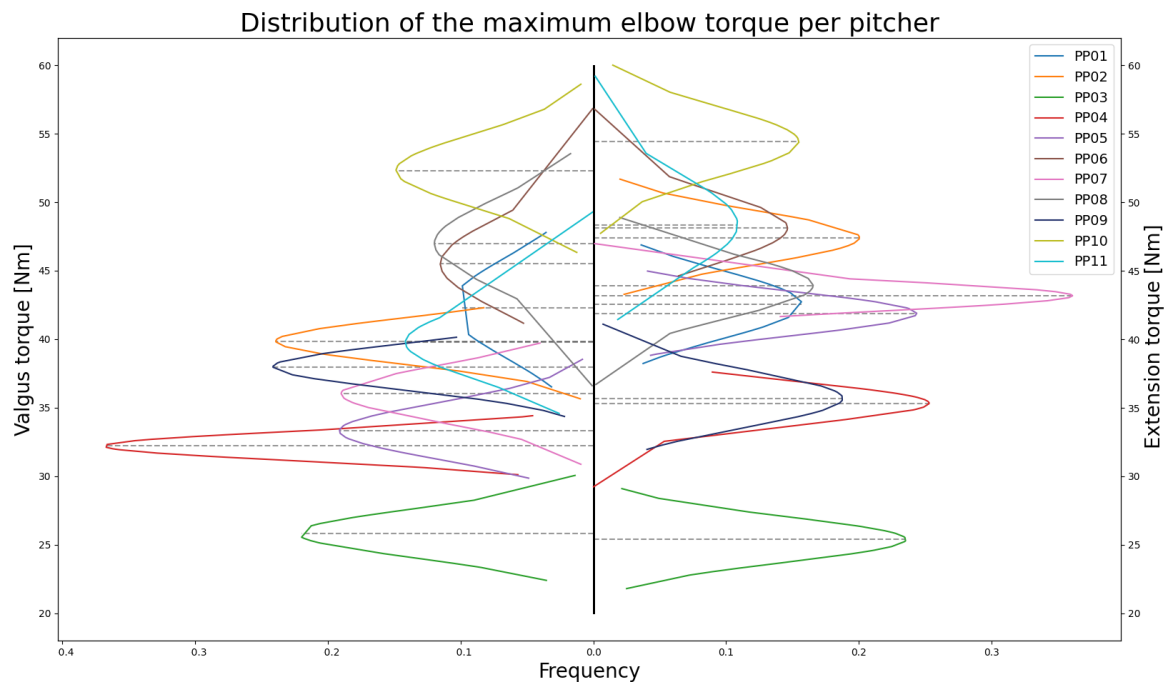
Distribution of the maximum elbow torque per pitcher

Figure 3: The maximum valgus (left) and extension (right) torque of each participant displayed as normal distributions.

The valgus torque and extension torque

Over all the pitches performed within this research, considering which pitch belongs to which participant, the maximum valgus torque and extension torque are significantly positively correlated ($p=0.00$, $r^2=0.31$), see Figure 4 (black-dotted line). The standard deviation of the valgus torque and the standard deviation of the extension torque are also significantly positively correlated ($p=0.04$, corr=0.63, see Table 2).

Figure 4 shows the relationship between the maximum valgus and extension torque both within and between participants. First, within participants the elbow torques of the performed pitches per participant are displayed, each in a corresponding colour to their thrower. Next, the linear regression result is shown as a line through each participant's pitches (see Appendix B, Table 2 for individual results). The participants whose elbow torques are significantly correlated are marked in the legend with 'p<0.05'. At last, for each participant, an ellipse is drawn with a width of the extension torque's standard deviation and a height of the valgus torque's standard deviation, representing the within-pitcher variability. Between-pitcher variability is quantified in comparison to the linear regression with a panel analysis, displayed as the black-dotted line.

The relationship between the elbow torques and ball speed

The maximum valgus torque and ball speed of all the performed pitches, considering the panel analysis, are significantly positively correlated, but with a low correlation ($p=0.00$, $r^2 = 0.15$). Figure 5 is built up similarly to Figure 4. The figure shows that between-pitcher variability is high. This is visible when comparing two participants with roughly the same ball speed, for example, participant
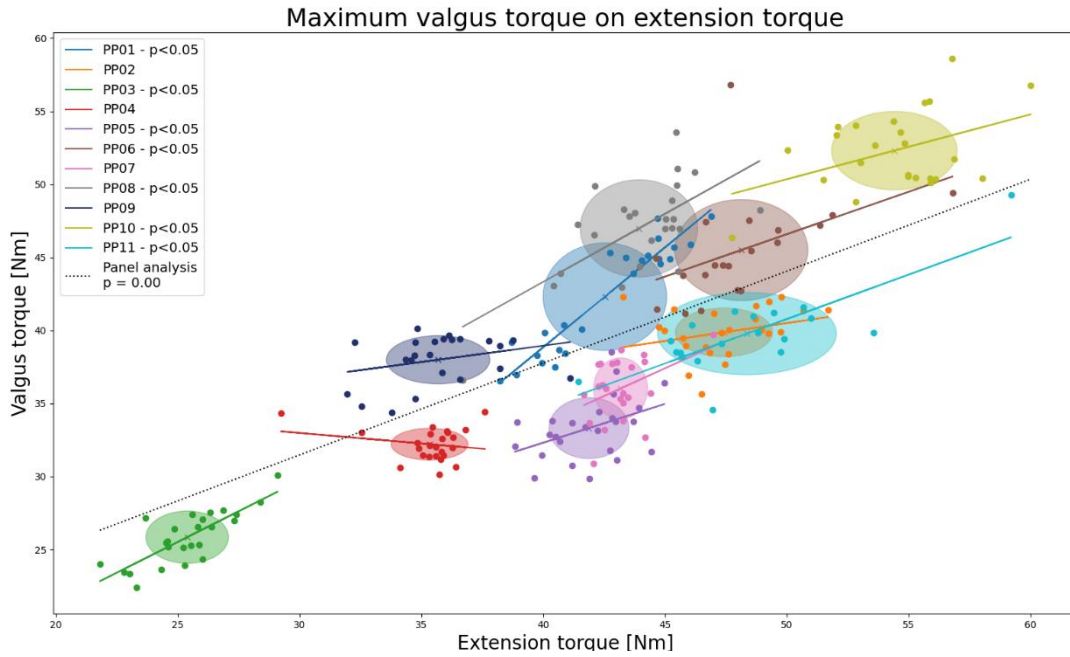
7

Figure 4: Linear regression of the maximum valgus torque on the maximum extension torque for each participant (colours) (those significant, legend labels 'p<0.05') and over the whole group with a panel analysis (black, dotted). The ellipses are of the size of the standard deviations.

five and participant eight. While the ball speed is almost equal, the difference in applied mean maximum valgus torque is approximately 15 Nm. The other way around, when, for example, comparing participant six and participant eight, with almost the same applied valgus torque, we see a difference in ball speed of approximately 4 mph. Evaluating the results within each participant, the legend shows (p<0.05) at which participants a correlation was present between the maximum valgus torque and ball speed. These participants have a higher r^2 than the participants where no significant correlation appears (see Appendix B, Table 3 for individual results). The valgus torque's standard deviation is not correlated to the ball speed (p=0.30, corr=0.35, Table 2).
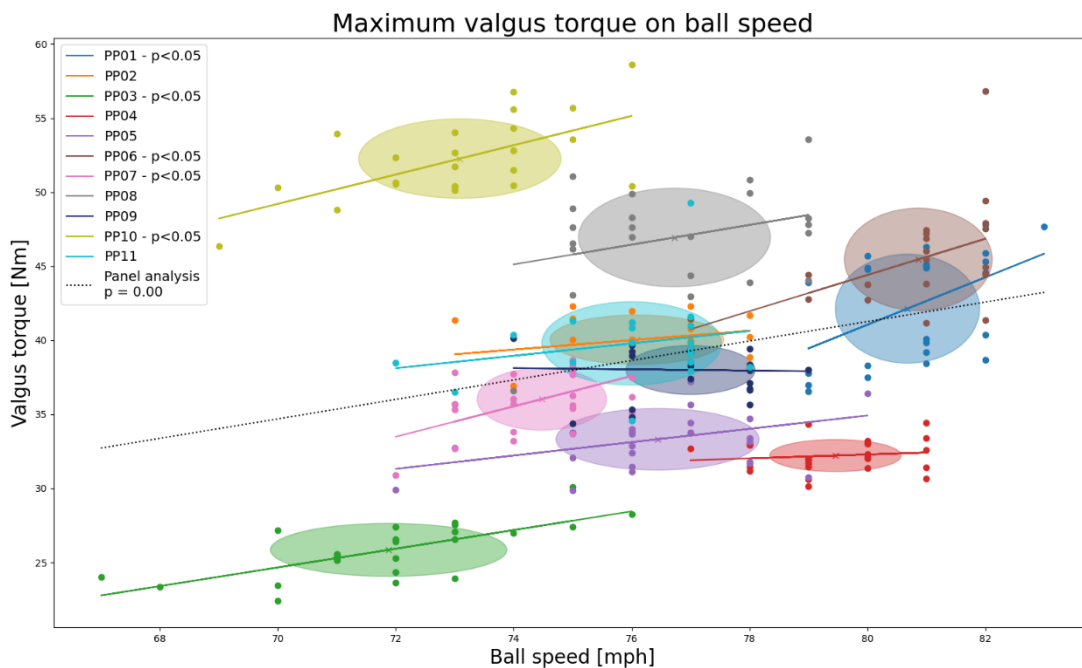

Figure 5: Linear regression of the maximum valgus torque on the ball speed for each participant (colours) (those significant, legend labels 'p<0.05') and over the whole group with a panel analysis (black, dotted). The ellipses are of the size of the standard deviations.
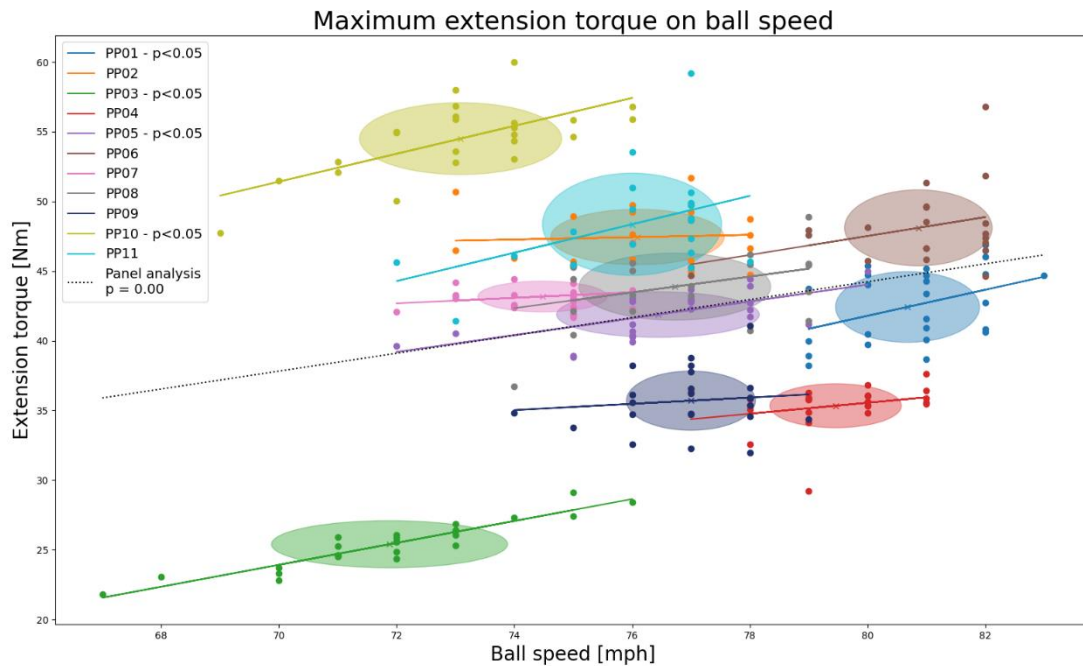
Figure 6: Linear regression of the maximum extension torque on the ball speed for each participant (colours) (those significant, legend labels 'p<0.05') and over the whole group with a panel analysis (black, dotted). The ellipses are of the size of the standard deviations.

The maximum extension torque and the ball speed, applying a panel analysis over all pitches, are significantly positively correlated, but the r^2 is small (p=0.00, r^2=0.17) (an equal method used as Figure 4). A high between-pitcher variability is evident when comparing participant three with participant ten; their ball speeds differ only 1 mph, where their applied extension torques differ almost 30 Nm (Figure 6). For a specific extension torque, the ball speed cannot be predicted precisely either, as becomes visible when comparing participant six and eight. Their applied extension torque is approximately 48 Nm, but their performed ball speed is respectively 81 and 76 mph. Within the participants, those where a significant correlation is found between maximum extension torque and ball speed are named in the legend (p<0.05). These participants have a higher r^2 than those where the correlation is not significantly present (see Appendix B, Table 4 for individual results). Between the participants, the standard deviation of the extension torque is not significantly correlated to the ball speed (p=0.51, corr=0.22, Table 2).

When comparing the magnitude and the standard deviation of the ball speed, a significantly negative correlation is found (p=0.03, corr=-0.65, Table 2).

Table 2: Linear regressions performed on standard deviations (SD) and average magnitudes (Mag) of parameters (n=11). Reporting p-value (underlined is significant) and Pearson correlation.

Dependent (Y)	Independent (X)	p-value	Correlation
SD valgus	SD extension	0,04	0,63
SD valgus	Mag ball	0,30	0,35
SD extension	Mag ball	0,51	0,22
SD valgus	Mag valgus	0,02	0,67
SD extension	Mag extension	0,11	0,51
SD ball	Mag ball	0,03	-0,65

Discussion

The aim of this study was to investigate the elbow torques and corresponding variability during a fastball pitch and determine if the magnitude and within-pitcher variability were related. Furthermore, the aim was to determine if there was a relationship between the elbow torques and the ball speed. Within-pitcher variability differed among participants, making it discouraged to select only one pitch per pitcher since this one pitch will not represent all the performed pitches, especially not if the fastest is selected. The valgus torque and the within-pitcher variability are both expected to influence the risk for an injury. This study showed the importance of evaluating the results of each participant individually.

The fact that within-pitcher variability is present, varies between participants, and is not neglectable is confirmed by the presence of the ellipses in Figures 4, 5, and 6 and by Figure 3, as was already assumed by some previous researches (Aguinaldo & Chambers, 2009; Fleisig et al., 1995). An example of the differing variability per participant is found when comparing participant two and participant eleven. Their average maximum valgus torque, maximum extension torque, and ball speed are each almost equal (see Table 1), but their within-pitcher load variability (of the valgus and extension torque) is certainly different. This result confirms that taking only one (or a few) pitch per pitcher into consideration is not representative for that pitcher's performance or characteristics. This study found that, when comparing pitchers with each other, the within-pitcher load variability and the corresponding maximum elbow torques are related. This means that if a pitcher throws with a higher average maximum elbow torque compared to other pitchers, the within-pitcher load variability is also expected to be higher compared to other pitchers.

According to previous research, an increased valgus torque is considered to lead to an increased UCL injury risk (Aguinaldo & Chambers, 2009; Sabick et al., 2004; Wilk et al., 2014). Since the within-pitcher load variability and applied valgus torque between pitchers are related, it is expected that the variability can also be related to a UCL injury risk. It should be noted that the assumption was made that the valgus torque can serve as a proxy for the UCL load and the valgus torque within-pitcher variability as a proxy for the within-pitcher load variability of the UCL. The expectation that the variability and UCL injury risk are related, is in line with the model made by van Trigt et al. (2020), who assumed that a higher within-pitcher variability would increase the risk for an injury (van Trigt et al., 2020). Finding the presence and influence of this within-pitcher valgus torque variability emphasises the need for more research on within-pitcher variability since the current study is performed on just eleven participants.

The valgus and extension torque are positively correlated, emphasising the compromise between performance and injury risk. The average maximum valgus torque found in this study is relatively low compared to the valgus torque found in previous research. The average maximum extension torque is higher compared to the maximum valgus torque, where previous research found the opposite: a higher valgus torque than extension torque (Fleisig et al., 1999; Gasparutto et al., 2016, 2021; Okoroha et al., 2018). Possible explanations for the differences in ratio between the valgus and extension torque might be the definition of the local coordinate system. Other researchers might have split up the elbow torque in a different manner, like splitting it up into two components instead of three as this study did. If, for example, the torque in the pronation-supination direction is combined with the torque in the flexion-extension direction, it could explain the discrepancy of the ratios. Different measuring techniques (for example: camera, opto-tracking, IMU) might lead to different position data accuracy, potentially causing a local coordinate system that does not precisely match the actual anatomical coordinate system, which could clarify the ratio difference.

Since no two researches are identical, it is difficult to compare the results. Further research should examine if studies, with a similar setup, will find different valgus torques, extension torques, and within-pitcher load variability.

Even though ball speed is an easy-to-measure parameter and often used to measure performance, the high between-pitcher variability and the low r^2 demonstrate that when comparing the participants to the whole group, the ball speed is not a suitable predictor for the elbow torques (and neither are the elbow torques a good predictor for the ball speed). The participants who had a correlation between the elbow torque and the ball speed showed a higher r^2 than those where no correlation was present. This demonstrates that if a correlation occurs individually, the ball speed can serve as a predictor for the elbow torque. A study from Slowik et al. (2019) found similar differences between-pitchers and within-pitchers concerning the prediction of the elbow torque with the ball speed (Slowik et al., 2019). From these results, we can conclude that more insight into a pitcher's behaviour and performance is given when each participant is considered individually instead of only analysing each participant with the whole group.

This study compromised two minor limitations. The first limitation is that the group size was relatively small (n=11). The linear regression between the maximum extension torque and the corresponding within-pitcher variability was near-significant (p=0.11), nevertheless, this study still assumed that if the maximum extension torque increases the corresponding within-pitcher variability will increase simultaneously.
The second limitation is that not for all participants 25 pitches could be used for analysis (Appendix B, Table 1 shows which pitches were excluded). Future research should be conducted where desirably each participant would throw as many pitches as allowed of which eventually for each participant the same number of pitches can be selected based on data quality. Improvements at the motion analysis can also help reduce the number of excluded pitches. However, the baseball pitch motion is so fast that tracking all the markers and not losing a marker is a challenging task.
There is not a specific minimum number of pitches required for a good analysis. Comparing normal distributions of the elbow torques (like Figure 3) when different number of maximum pitches per participant are considered (see Appendix B, Figures 3-5 for the comparison), shows that the assumption can be made that the participant with the least number of pitches in this study (19 pitches) is still suitable for determining and evaluating the within-pitcher variability.

As previously stated, the valgus torque and variability are assumed in this study to be representative for the load and load variability on the UCL. This study has been performed on a segment level. To gain more insight into the specific loading of the UCL, similar research should be executed on a ligament level. A musculoskeletal model should be used to perform ligament level research, where the use of the Delft Elbow and Shoulder Model (DSEM) is advised (Hordijk, 2017; Nikooyan et al., 2011). See Appendix C for more information.
The relationship between the valgus torque and injury risk is often named in this study. However, the injury risk was not examined. Further research is needed, performed over a more extended period of time and considering both the injury rate and the within- and between-variability among the pitchers, to compare results with this study and to determine whether the expectation of this study that the within-pitcher variability and a UCL injury are related is valid.

Valgus torque, extension torque, variability and ball speed are not the only proxies existing for baseball pitching performance and injury risk. The current study could be extended with other

parameters of interest, or current parameters could be replaced to gain more knowledge on baseball pitching.

For example, this study only investigated the elbow torques and ball speed when performing a fastball pitch. Other pitch types come with their own trajectory and corresponding kinematics and kinetics (Fortenbaugh et al., 2009). Similar research performed with other pitch types should establish if similar correlations between the valgus and extension torque and between the magnitude and variability of the elbow torques are present. If different results appear, a recommendation could be made to encourage certain pitch types above others.

A study by Okoroha et al. (2018) reported that when fatigue develops, a decrease in ball speed occurred and an increase in applied external valgus torque (Okoroha et al., 2018). Furthermore, fatigue is found to influence the risk for an injury (Olsen et al., 2006; Yang et al., 2014). Executing a similar study as this paper described, but with the additional measurement of fatigue, can give an insight into whether fatigue could be related to an increased level of variability.

Conclusion

Throwing with a higher maximum elbow torque results in a higher within-pitcher load variability in comparison to other pitchers. Considering this result, both the magnitude and the within-pitcher load are expected to be related to injury risk. Since within-pitcher variability is present and differs among pitchers, this study discourages to consider only one (or a few) pitch per pitcher because this cannot represent all the pitches of that pitcher, especially not if just the fastest is chosen. When comparing the pitchers among each other, the ball speed is not a good indicator for the applied elbow torque. When a correlation between an elbow torque and ball speed is present within a pitcher, the ball speed can serve as an indicator for that elbow torque of the pitcher. This emphasises the importance of investigating the results within a pitcher instead of only comparing them to the whole group.

References

Adler, D. (2019). *Identifying pitch types: A fan's guide*. MLB. https://www.mlb.com/news/identifying-pitch-types-a-fan-s-guide

Aguinaldo, A. L., & Chambers, H. (2009). Correlation of Throwing Mechanics With Elbow Valgus Load in Adult Baseball Pitchers. *The American Journal of Sports Medicine2*, *37*(10), 2043–2048. https://doi.org/10.1177/0363546509336721

Anz, A. W., Bushnell, B. D., Griffin, L. P., Noonan, T. J., Torry, M. R., & Hawkins, R. J. (2010). Correlation of torque and elbow injury in professional baseball pitchers. *American Journal of Sports Medicine*, *38*(7), 1368–1374. https://doi.org/10.1177/0363546510363402

Bartlett, R., Wheat, J., & Robins, M. (2007). Is movement variability important for sports biomechanists? *Sports Biomechanics*, *6*(2), 224–243. https://doi.org/10.1080/14763140701322994

Brooks, M. (2020). *How to identify the most common pitches in baseball: spin, speed & location.* Applied Vision Baseball. https://appliedvisionbaseball.com/how-to-identify-pitch-types-spin-speed-location/

Buffi, J. H., Werner, K., Kepple, T., & Murray, W. M. (2015). Computing Muscle, Ligament, and Osseous Contributions to the Elbow Varus Moment During Baseball Pitching. *Annals of Biomedical Engineering*, *43*(2), 404–415. https://doi.org/10.1007/s10439-014-1144-z

Bushnell, B. D., Anz, A. W., Noonan, T. J., Torry, M. R., & Hawkins, R. J. (2010). Association of Maximum Pitch Velocity and Elbow Injury in Professional Baseball Pitchers. *American Journal of Sports Medicine*, *38*(4), 728–732. https://doi.org/10.1177/0363546509350067

Conte, S. A., Requa, R. K., & Garrick, J. G. (2001). Disability days in Major League Baseball. *American Journal of Sports Medicine*, *29*(4), 431–436. https://doi.org/10.1177/03635465010290040801

Davids, K., Glazier, P., Araujo, D., & Bartlett, R. (2003). Movement Systems as Dynamical Systems. *Sports Medicine*, *33*(4), 245–260. https://doi.org/10.2165/00007256-200333040-00001

de Leva, P. (1996). Adjustments to Zatsiorsky-Seluyanov's segment inertia parameters. *Journal of Biomechanics*, *29*(9), 1223–1230.

Dillman, C. I., Fleisig, G. S., & Andrews, J. R. (1993). Biomechanics of Pitching with Emphasis upon Shoulder Kinematics. *Journal of Orthopaedic & Sports Physical Therapy*, *18*(2), 402–408.

Feltner, M., & Dapena, J. (1986). Dynamics of the shoulder and elbow joints of the throwing arm during a baseball pitch. *International Journal of Sport Biomechanics*, *2*, 235–259.

Fleisig, G. S., Andrews, J. R., Dillman, C. I., & Escamilla, R. F. (1995). Kinetics of Baseball Pitching with implications about injury prevention. *The American Journal of Sports Medicine*, *23*(2), 233–239.

Fleisig, G. S., Barrentine, S. W., Zheng, N., Escamilla, R. F., & Andrews, J. R. (1999). Kinematic and kinetic comparison of baseball pitching among various levels of development. *Journal of Biomechanics*, *32*(12), 1371–1375. https://doi.org/10.1016/S0021-9290(99)00127-X

Fleisig, G. S., Kingsley, D. S., Loftice, J. W., Dinnen, K. P., Ranganathan, R., Dun, S., Escamilla, R. F., & Andrews, J. R. (2006). Kinetic comparison among the fastball, curveball, change-up, and slider in collegiate baseball pitchers. *American Journal of Sports Medicine*, *34*(3), 423–430. https://doi.org/10.1177/0363546505280431

Fortenbaugh, D., Fleisig, G. S., & Andrews, J. R. (2009). Baseball pitching biomechanics in relation to injury risk and performance. *Sports Health*, *1*(4), 314–320. https://doi.org/10.1177/1941738109338546

Gasparutto, X., van der Graaff, E., van der Helm, F. C. T., & Veeger, D. H. E. J. (2021). Influence of biomechanical models on joint kinematics and kinetics in baseball pitching. *Sports Biomechanics*, *20*(1), 96–108. https://doi.org/10.1080/14763141.2018.1523453

Gasparutto, X., Van Der Graaff, E., Van Der Helm, F. C. T., & Veeger, H. E. J. (2016). Elite Athlete Motor and Loading Actions on the Upper Limb in Baseball Pitching. *Procedia Engineering*, *147*, 181–185. https://doi.org/10.1016/j.proeng.2016.06.210

Gough, C. (2018). *Number of participants in baseball in the United States from 2006 to 2017 (in millions)*. Outdoor Participant Report. https://doi.org/10.15439/2019F121

Hordijk, P. (2017). *Musculoskeletal modelling of the shoulder during baseball pitching*. http://resolver.tudelft.nl/uuid:22c986dd-b42d-4581-b7da-58039ab06e90

Hurd, W. J., Kaufman, K. R., & Murthy, N. S. (2011). Relationship between the medial elbow adduction moment during pitching and ulnar collateral ligament appearance during magnetic resonance imaging evaluation. *American Journal of Sports Medicine*, *39*(6), 1233–1237. https://doi.org/10.1177/0363546510396319

Lin, F., Kohli, N., Perlmutter, S., Lim, D., Nuber, G. W., & Makhsous, M. (2007). Muscle contribution to elbow joint valgus stability. *Journal of Shoulder and Elbow Surgery*, *16*(6), 795–802. https://doi.org/10.1016/j.jse.2007.03.024

Nikooyan, A. A., Veeger, H. E. J., Chadwick, E. K. J., Praagman, M., & Van Der Helm, F. C. T. (2011). Development of a comprehensive musculoskeletal model of the shoulder and elbow. *Medical and Biological Engineering and Computing*, *49*(12), 1425–1435. https://doi.org/10.1007/s11517-011-0839-7

Okoroha, K. R., Meldau, J. E., Lizzio, V. A., Meta, F., Stephens, J. P., Moutzouros, V., & Makhni, E. C. (2018). Effect of Fatigue on Medial Elbow Torque in Baseball Pitchers: A Simulated Game Analysis. *American Journal of Sports Medicine*, *46*(10), 2509–2513. https://doi.org/10.1177/0363546518782451

Olsen, S. J., Fleisig, G. S., Dun, S., Loftice, J., & Andrews, J. R. (2006). Risk factors for shoulder and elbow injuries in adolescent baseball pitchers. *American Journal of Sports Medicine*, *34*(6), 905–912. https://doi.org/10.1177/0363546505284188

Pappas, A., Zawacki, R., & Sullivan, T. (1985). Biomechanics of baseball pitching. *American Journal of Sports Medicine*, *13*(4), 216–222.

Posner, M., Cameron, K. L., Wolf, J. M., Belmont, P. J., & Owens, B. D. (2011). Epidemiology of major league baseball injuries. *American Journal of Sports Medicine*, *39*(8), 1676–1680. https://doi.org/10.1177/0363546511411700

Roegele, J. (2018). *Tommy John surgery list. Hardball Times.* https://docs.google.com/spreadsheets/d/1gQujXQQGOVNaiuwSN680Hq-FDVsCwvN-3AazykOBON0/edit#gid=0

Sabick, M. B., Torry, M. R., Lawton, R. L., & Hawkins, R. J. (2004). Valgus torque in youth baseball pitchers: A biomechanical study. *Journal of Shoulder and Elbow Surgery*, *13*(3), 349–355. https://doi.org/10.1016/j.jse.2004.01.013

Scarborough, D. M., Bassett, A. J., Mayer, L. W., & Berkson, E. M. (2018). Kinematic sequence patterns in the overhead baseball pitch. *Sports Biomechanics*, *00*(00), 1–18. https://doi.org/10.1080/14763141.2018.1503321

Sheppard, K. (2021). *Linear models package* (4.21). https://doi.org/10.5281/zenodo.4588352

Slowik, J. S., Aune, K. T., Diffendaffer, A. Z., Lyle Cain, E., Dugas, J. R., & Fleisig, G. S. (2019). Fastball velocity and elbow-varus torque in professional baseball pitchers. *Journal of Athletic Training*, *54*(3), 296–301. https://doi.org/10.4085/1062-6050-558-17

Sports show. (2020). *Top 10 Most Popular Sports in America 2020 (TV Ratings)*. https://sportsshow.net/most-popular-sports-in-america/

Stodden, D. F., Fleisig, G. S., McLean, S. P., & Andrews, J. R. (2005). Relationship of biomechanical factors to baseball pitching velocity: Within pitcher variation. *Journal of Applied Biomechanics*, *21*(1), 44–56. https://doi.org/10.1123/jab.21.1.44

Stodden, D. F., Fleisig, G. S., McLean, S. P., Lyman, S. L., & Andrews, J. R. (2001). Relationship of pelvis and upper torso kinematics to pitched baseball velocity. *Journal of Applied Biomechanics*, *17*(2), 164–172. https://doi.org/10.1123/jab.17.2.164

Van Rossum, G., & Drake, F. L. (2009). *Python 3 Reference Manual* (3.7).

van Trigt, B., Leenen, T. A. J. R., Hoozemans, M. M. J. M., & van der Helm, F. F. C. T. (2020). Are UCL injuries a matter of bad luck ? The role of variability and fatigue quantified. *Proceedings*, *49*, 107. https://doi.org/10.3390/proceedings2020049107

van Trigt, B., Vliegen, L., Leenen, T., & Veeger, D. (2021). The ulnar collateral ligament loading

paradox between in-vitro and in-vivo studies on baseball pitching: narrative review. *International Biomechanics*. In press.

Virtanen, P., Gommers, R., Oliphant, T. E., Haberland, M., Reddy, T., Cournapeau, D., Burovski, E., Peterson, P., Weckesser, W., Bright, J., van der Walt, S. J., Brett, M., Wilson, J., Millman, K. J., Mayorov, N., Nelson, A. R. J., Jones, E., Kern, R., Larson, E., … Contributors., S. 1. . (2020). SciPy 1.0: Fundamental Algorithms for Scientific Computing in Python. *Nature Methods*, *17*(3), 261–272.

Wilk, K. E., Macrina, L. C., Fleisig, G. S., Aune, K. T., Porterfield, R. A., Harker, P., Evans, T. J., & Andrews, J. R. (2014). Deficits in Glenohumeral Passive Range of Motion Increase Risk of Elbow Injury in Professional Baseball Pitchers A Prospective Study. *The American Journal of Sports Medicine*, *42*(9), 2075–2081. https://doi.org/10.1177/0363546514538391

Wu, G., Van Der Helm, F. C. T., Veeger, H. E. J., Makhsous, M., Van Roy, P., Anglin, C., Nagels, J., Karduna, A. R., McQuade, K., Wang, X., Werner, F. W., & Buchholz, B. (2005). ISB recommendation on definitions of joint coordinate systems of various joints for the reporting of human joint motion - Part II: Shoulder, elbow, wrist and hand. *Journal of Biomechanics*, *38*(5), 981–992. https://doi.org/10.1016/j.jbiomech.2004.05.042

Yang, J., Mann, B. J., Guettler, J. H., Dugas, J. R., Irrgang, J. J., Fleisig, G. S., & Albright, J. P. (2014). Risk-prone pitching activities and injuries in youth baseball: Findings from a national sample. *American Journal of Sports Medicine*, *42*(6), 1456–1463. https://doi.org/10.1177/0363546514524699

Zatsiorsky, V. M. (1990). Methods of determing mass-inertial characteristics of human body segments. *Contemporasy Problems of Biomechnics*, 272–291.

Zatsiorsky, V. M. (2002). *Kinetics of Human Motion*. Human Kinetics.

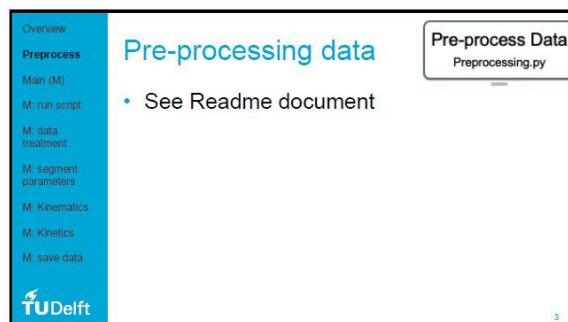## Appendix A – 3D Inverse dynamics python model

This following PowerPoint slides provide information on the structure and content of the 3D inverse dynamics upper extremity Python model, made by Van Trigt, Leenen, and Bouman.
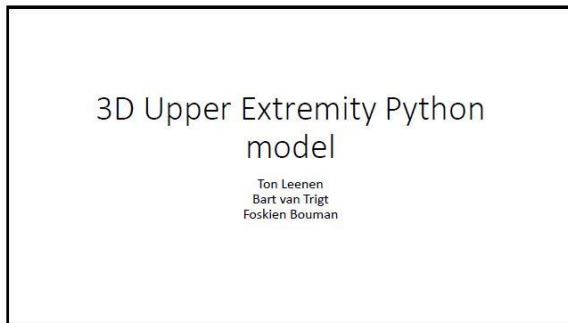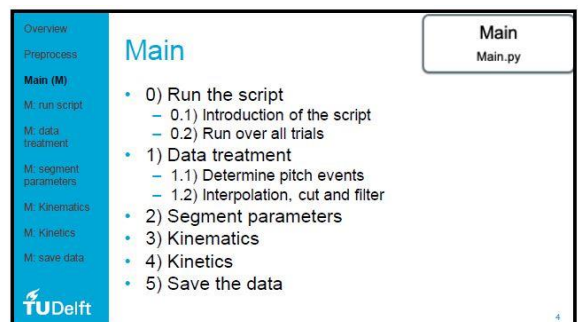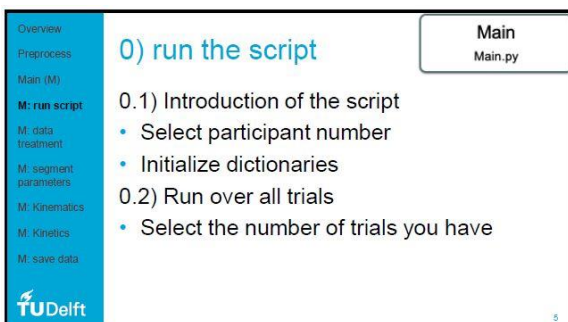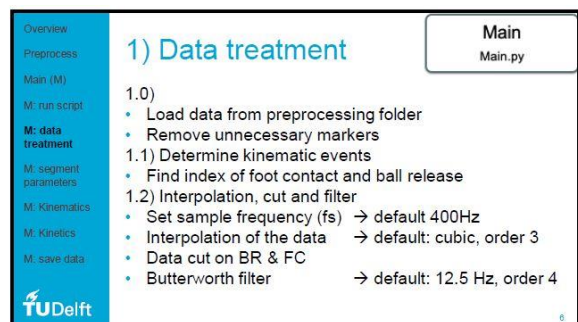

1
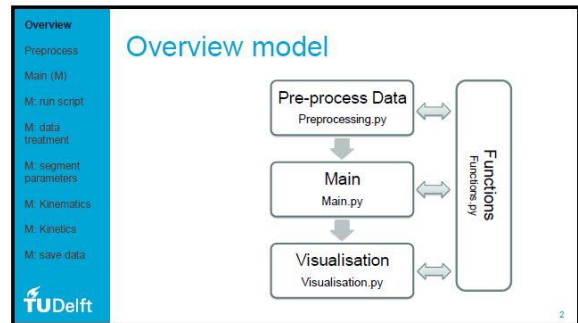
2

3

4

5

6

Slide 7

Overview
Preprocess
Main (M)
M: run script
M: data treatment
M: segment parameters
M: Kinematics
M: Kinetics
M: save data

Main
Main.py

2) Segment parameters

- 2.1) Pelvis
- 2.2) Trunk
- 2.3) Upper arm
- 2.4) Forearm
- 2.5) Hand

*TU*Delft

7

Slide 8

Overview
Preprocess
Main (M)
M: run script
M: data treatment
M: segment parameters
M: Kinematics
M: Kinetics
M: save data

Main
Main.py

Segment calculations

- Determine body segment parameters for each body segment separately in global.
- Calculate these segment parameters with the pitch motion (seg_{motion}).

Segment parameters:
- Joint centers
- Mass
- CoM
- Origin
- Velocity
- Acceleration
- Angular velocity segment
- Angular velocity global
- Angular acceleration global
- Global rotation matrix
- Global translation matrix
- Global inertia tensor
- Principal moment of inertia

*TU*Delft

8

Slide 9

Overview
Preprocess
Main (M)
M: run script
M: data treatment
M: segment parameters
M: Kinematics
M: Kinetics
M: save data

General calculations

- From axis-definition compose *gRseg* and *gTseg*.
- Determine with Zatsiorsky parameters: *CoM*, *segment length* and *regression parameters*.
- Calculate *mass* and *inertia matrix* (with: reg_{par}, seg_{length}, *circumference*).
- *Inertia tensor* from *inertia matrix* and *gRseg*.
- Calculate $v_{seg}\left(=\frac{d(CoM)}{dt}\right)$ & $a_{seg}\left(=\frac{d(v_{seg})}{dt}\right)$.
- Calculate *avSeg* & *alfaSeg* via skew-symmetric method.

*TU*Delft

9

Slide 10

Overview
Preprocess
Main (M)
M: run script
M: data treatment
M: segment parameters
M: Kinematics
M: Kinetics
M: save data

Functions
Functions.py

2.1 pelvis

Input: RSIAS, LSIAS, RSIPS, and LSIPS.
Hip joint centers according to Bell, 1999, and Leardini, 1999.
$origin = \frac{LSIAS + RSIAS}{2}$. $CoM = X, Y, Z$ with De Leva, 1996.

Axis (all normalized):
$QTP = cross(\frac{LSIPS + RSIPS}{2} - origin, LSIAS - origin)$.
$z_{axis} = LSIAS - RSIAS$
$x_{axis} = cross(QTP, z_{axis})$.
$y_{axis} = cross(z_{axis}, x_{axis})$.

*TU*Delft

10

Slide 11

Overview
Preprocess
Main (M)
M: run script
M: data treatment
M: segment parameters
M: Kinematics
M: Kinetics
M: save data

Functions
Functions.py

2.2) trunk

Input: IJ, PX, C7, and T8.
No joint centers.
Origin = IJ. $CoM = X, Y, Z$ with De Leva, 1996.

Axes (all normalized):
$QFP = cross(SJC - EJC, LHE) - EJC$.
$y_{axis} = SJC - EJC$.
$z_{axis} = cross(QFP, y_{axis})$.
$x_{axis} = cross(y_{axis}, z_{axis})$.

*TU*Delft

11

Slide 12

Overview
Preprocess
Main (M)
M: run script
M: data treatment
M: segment parameters
M: Kinematics
M: Kinetics
M: save data

Functions
Functions.py

2.3) Upper arm

Input: LHE, MHE, and AC.
$EJC = \frac{LHE + MHE}{2}$, SJC = AC +(EJC-AC)*de Leva, 1996
origin = EJC.
$CoM = SJC + (EJC - SJC) * Zatsiorsky$.

Axes (all normalized):
$z_{temp} = LHE - MHE$ (assuming right − handedness).
$y_{axis} = SJC - EJC$.
$x_{axis} = cross(y_{axis}, z_{temp})$.
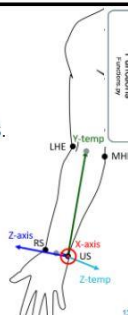$z_{axis} = cross(x_{axis}, y_{axis})$.

*TU*Delft

12

Slide 13

Overview
Preprocess
Main (M)
M: run script
M: data treatment
M: segment parameters
M: Kinematics
M: Kinetics
M: save data

Functions
Functions.py

2.4 Forearm

Input: LHE, MHE, US and RS.
$WJC = \frac{US + RS}{2}$, $EJC = \frac{LHE + MHE}{2}$, origin = US.
$CoM = EJC + (US - EJC) * Zatsiorsky$.

Axes (all normalized):
$z_{temp} = LHE - MHE$ (assuming right).
$y_{axis} = EJC - US$.
$x_{axis} = cross(y_{axis}, z_{temp})$.
$z_{axis} = cross(x_{axis}, y_{axis})$.

*TU*Delft

13

Slide 14

Overview
Preprocess
Main (M)
M: run script
M: data treatment
M: segment parameters
M: Kinematics
M: Kinetics
M: save data

Functions
Functions.py

2.5) hand

Input: US, RS and MH3.
$WJC = \frac{US + RS}{2}$, origin = WJC.
$CoM = WJC + (MH3 - WJC) * Zatsiorsky$.
Axes (all normalized):
$z_{temp} = RS - WJC$.
$y_{axis} = WJC - MH3$.
$x_{axis} = cross(y_{axis}, z_{temp})$.
$z_{axis} = cross(x_{axis}, y_{axis})$.

*TU*Delft

14

Slide 15

Overview
Preprocess
Main (M)
M: run script
M: data treatment
M: segment parameters
M: Kinematics
M: Kinetics
M: save data

*TU*Delft

2) Segment parameters

Main
Main.py

- Combine all calculated segment parameters into one model, according to this format

15

Slide 16

Overview
Preprocess
Main (M)
M: run script
M: data treatment
M: segment parameters
M: Kinematics
M: Kinetics
M: save data

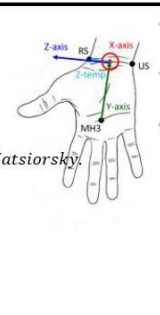*TU*Delft

3) Kinematics

- Calculate joint angles

16

Slide 17

Overview
Preprocess
Main (M)
M: run script
M: data treatment
M: segment parameters
M: Kinematics
M: Kinetics
M: save data

*TU*Delft

4) Kinetics

- 4.1) Global force
- 4.2) Global moment
- 4.3) Anatomical moment
- 4.4) Motor and stability moment

17

Slide 18

Overview
Preprocess
Main (M)
M: run script
M: data treatment
M: segment parameters
M: Kinematics
M: Kinetics
M: save data

*TU*Delft

4.1 Global force

Functions
Functions.py

Calculate using the Newton-Euler method

$$\sum F = F_{prox} + F_g + F_{dist} = m * a$$

$$F_{prox} = F_{ma} - F_g - F_{dist}$$

NB: $Distal = -Proximal$

18

Slide 19

Overview
Preprocess
Main (M)
M: run script
M: data treatment
M: segment parameters
M: Kinematics
M: Kinetics
M: save data

*TU*Delft

4.2 Global moment

(NB: $Distal = -Proximal$)

Functions
Functions.py

Use Newton-Euler, turning around CoM

$$\sum M = M_{prox} + M_{Fprox} - M_{Fdist} + M_{dist} = I * \alpha$$

$$M_{prox} = I * \alpha - M_{Fprox} - M_{Fdist} - M_{dist}$$

Where:

$$I * \alpha = \begin{bmatrix} I_{xx}\dot{\omega}_x \\ I_{yy}\dot{\omega}_y \\ I_{zz}\dot{\omega}_z \end{bmatrix} + \begin{bmatrix} 0 & -\omega_z & \omega_y \\ \omega_z & 0 & -\omega_x \\ -\omega_y & \omega_x & 0 \end{bmatrix} * \begin{bmatrix} I_{xx}\omega_x \\ I_{yy}\omega_y \\ I_{zz}\omega_z \end{bmatrix}$$

$$MF_{dist} = d_{CoM-JCp} \times F_{prox} \& MF_{dist} = d_{CoM-JCd} \times F_{dist}$$

19

Slide 20

Overview
Preprocess
Main (M)
M: run script
M: data treatment
M: segment parameters
M: Kinematics
M: Kinetics
M: save data

*TU*Delft

4.3 Anatomical moment

Functions
Functions.py

- Convert the global moments to the anatomical axis system using the rotation matrix

$$^{local}M = {}^{global}R_{local} * {}^{global}M$$

20

Slide 21

Overview
Preprocess
Main (M)
M: run script
M: data treatment
M: segment parameters
M: Kinematics
M: Kinetics
M: save data

*TU*Delft

4.4 Motor and stability moment

Functions
Functions.py

- The anatomical moment (lM) could be distributed to a motor and a stability moment

- $M_{motor} = \sqrt{lM_y^2 + lM_z^2}$

- $M_{stability} = \sqrt{norm(lM)^2 - M_{motor}^2}$

21

Slide 22

Overview
Preprocess
Main (M)
M: run script
M: data treatment
M: segment parameters
M: Kinematics
M: Kinetics
M: save data

*TU*Delft

5) Save the data

- Save the calculated moments and any other desired information as a binary code to use in other scripts using the function: *pickle*

22

Appendix B – Additional results

This appendix provides the sensitivity test for the filter selection, additional information of the participants and a comparison of elbow torque normal distributions with multiple number of pitches included, and more extended results of the linear regressions, especially for each participant individually.
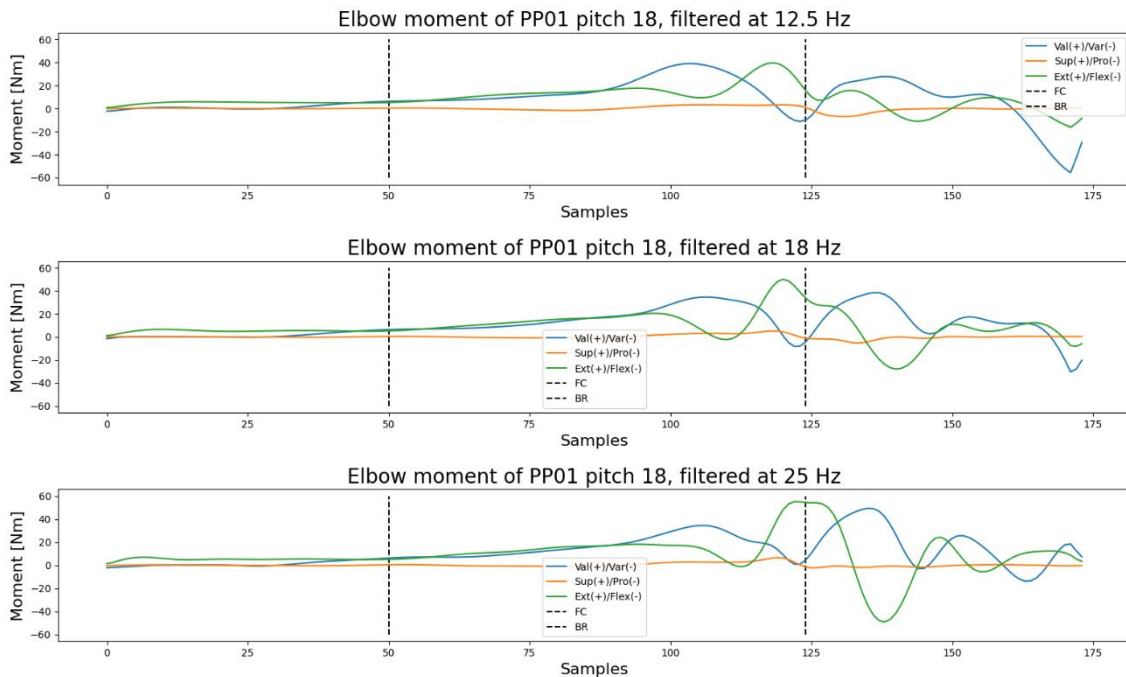
Filter sensitivity test

Figure 1: Sensitivity test of three cut-off frequencies (12.5, 18, and 25 Hz) when applying a 4th-order Butterworth filter on the elbow torque cut at 50 samples before ball release and 50 samples after foot contact (Participant 01, pitch 18).

At first, a small sensitivity test is performed to test the cut-off frequency to use for the 4th order Butterworth filter when filtering the raw input data. The effect of three cut-off frequencies are compared: 12.5, 18 and 25 Hz, based on the studies of Gasparutto et al. (2021), and Scarborough et al. (2018) who had a similar research setup (Gasparutto et al., 2021; Scarborough et al., 2018). The comparison was performed on the global elbow moment of two random selected pitches of different participants for a more substantiate result. The data was cut at 50 samples before *foot contact* and 50 samples after *ball release*, see Figure 1 and Figure 2 (*foot contact* and *ball release* are visualised by the black dotted lines).
The filter was selected where the least noise was visible but where the magnitude of the peak torques are the highest. From this sensitivity test the cut-off frequency of 12.5 Hz was selected.
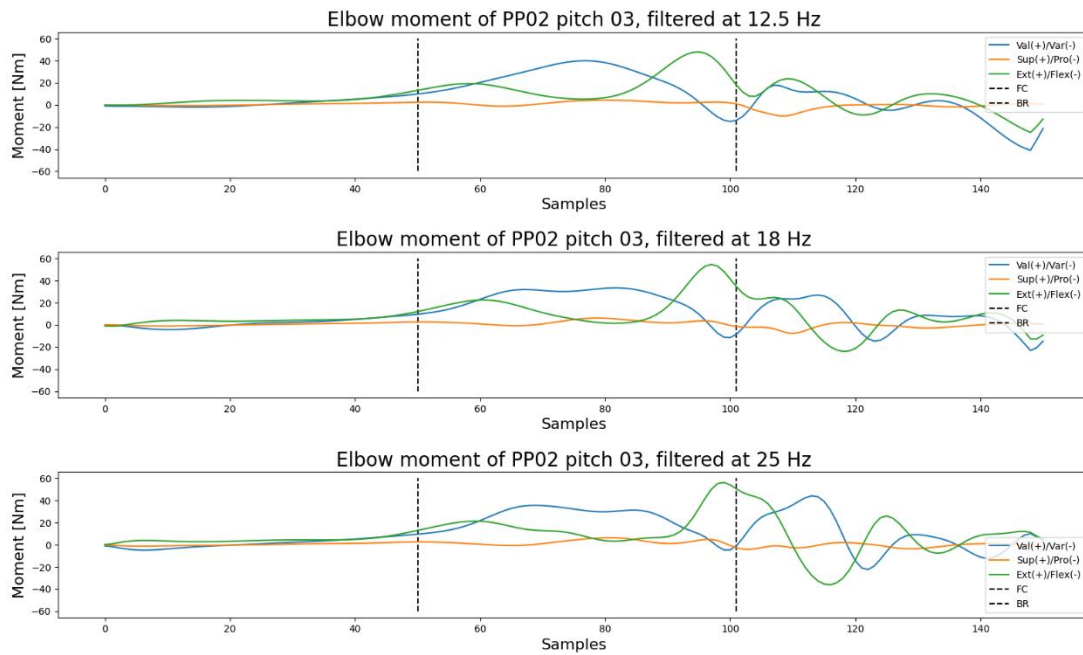
Figure 2: Sensitivity test of three cut-off frequencies (12.5, 18, and 25 Hz) when applying a 4th-order Butterworth filter on the elbow torque cut at 50 samples before ball release and 50 samples after foot contact (Participant 02, pitch 03).

Participant information

Secondly, Table 1 displays information on each participant. The first two rows show which pitches were excluded for each participant, based on the inclusion protocol explained in the method section. Additionally, the last two rows show the results from the Shapiro-Wilk test on the normality of the maximum valgus and extension torques of each participant. The maximum valgus or extension torques of a certain participant that is significantly normal distributed, is labeled with 'Yes', these where no significant normal distribution is found it is labeled with 'No'.

Table 1: Participant information on excluded pitches and the number of pitches left for analysis of each participant. Last two rows show if the maximum valgus and extension torques are significantly normal distributed.

Participants	Excluded pitches	Total pitches included	Normality of valgus torque	Normality of extension torque
PP01	14	24	No	Yes
PP02	-	25	Yes	Yes
PP03	-	25	Yes	Yes
PP04	21	24	Yes	No
PP05	-	25	Yes	Yes
PP06	02, 10, 12, 24, 25	20	No	No
PP07	18, 19	23	Yes	No
PP08	04	24	Yes	No
PP09	17, 18	23	No	Yes
PP10	03	24	Yes	Yes
PP11	08 (21-25)	19	No	Yes

Additionally, the normal distributions of the elbow torques are compared if different number of pitches are included. Of the maximum 25 pitches included for each participant, the normal distributions of the peak valgus torque and peak extension torque, subsequently 5, 10 or 15 pitches were, randomly chosen, excluded from the analysis, leaving a maximum of 20, 15 or 10 pitches for analysis. The results of these comparisons are displayed in Figures 3 (max n=20), 4 (max n=15), and 5 (max n=10).
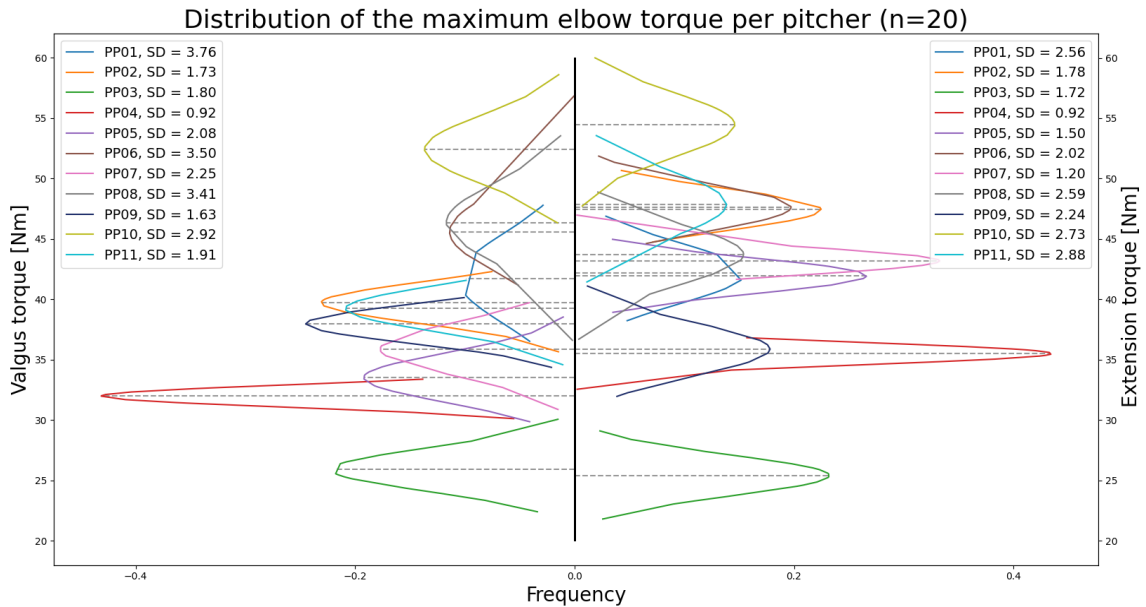

Figure 3: The maximum valgus (left) and extension (right) torque of each participant displayed as normal distributions, considering maximal 20 pitches per participant.
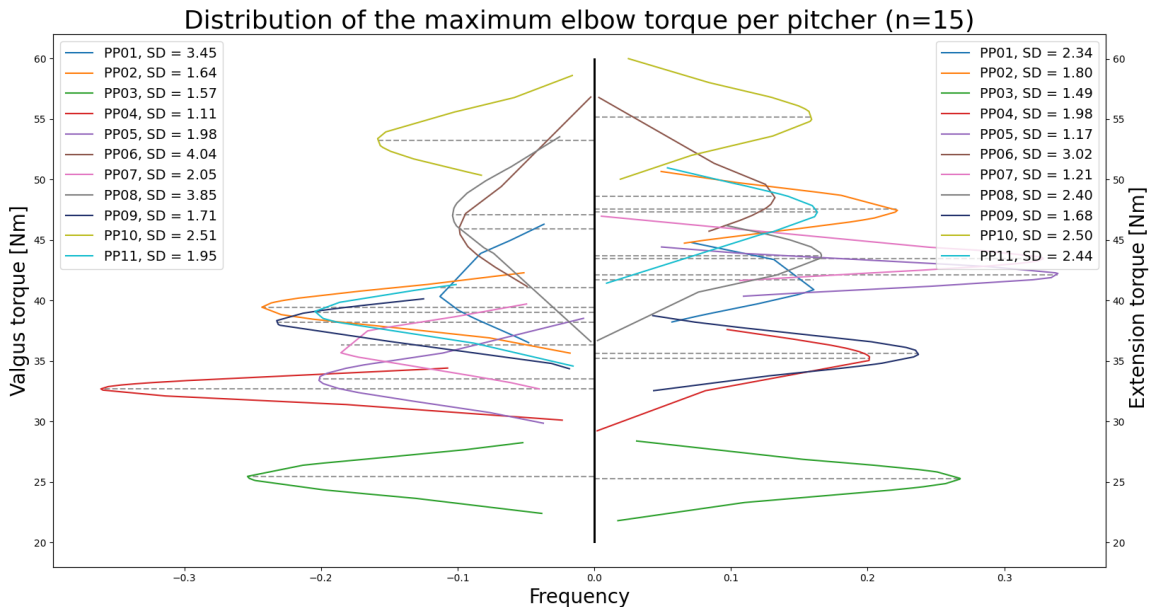
Figure 4: The maximum valgus (left) and extension (right) torque of each participant displayed as normal distributions, considering maximal 15 pitches per participant
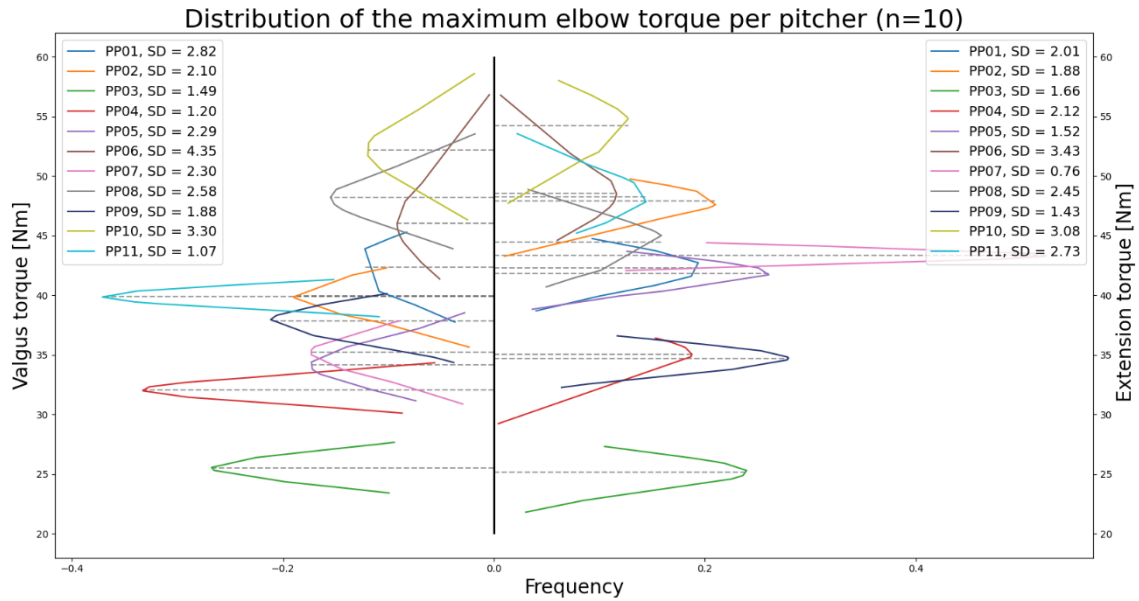
Figure 5: The maximum valgus (left) and extension (right) torque of each participant displayed as normal distributions, considering maximal 10 pitches per participant.

Linear regression results

At last, the extensive results of the statistical tests are displayed. The results of the individual linear regressions (p-value, coefficient, intersect, Pearson correlation) analysing the maximum valgus torque and the maximum extension torque, and each elbow torque with the ball speed are displayed in Table 2, 3, and 4. Table 5 shows the results (p-value, coefficient, intercept, and r^2) of the panel fixed effect ordinary least square analysis over all performed pitches, between the maximum valgus and extension torque, and between each elbow torques and the ball speed. The participants where the correlations are significant are underlined.

Table 2: Linear regression between maximum valgus torque and maximum extension torque for each participant. P-value (those significant are underlined), coefficient, intercept, and the Pearson's correlation is displayed.

Participant	p-value	Coefficient	Intercept	Correlation
PP01	0,00	1,37	-15,85	0,94
PP02	0,16	0,25	28,23	0,29
PP03	0,00	0,84	4,50	0,79
PP04	0,33	-0,14	37,30	-0,21
PP05	0,04	0,53	11,05	0,42
PP06	0,04	0,58	17,55	0,46
PP07	0,06	0,76	3,24	0,40
PP08	0,00	0,93	6,05	0,67
PP09	0,18	0,22	30,03	0,29
PP10	0,04	0,44	28,15	0,43
PP11	0,00	0,61	10,36	0,79

22

Table 3: Linear regression between maximum valgus torque and ball speed for each participant.
P-value (those significant are underlined), coefficient, intercept, and the Pearson's correlation is displayed.

Participant	p-value	Coefficient	Intercept	Correlation
PP01	0,02	1,60	-86,96	0,49
PP02	0,21	0,32	15,81	0,28
PP03	0,00	0,63	-19,49	0,71
PP04	0,53	0,13	21,82	0,13
PP05	0,07	0,45	-1,11	0,37
PP06	0,04	1,22	-53,36	0,46
PP07	0,01	1,03	-40,33	0,54
PP08	0,16	0,67	-4,20	0,31
PP09	0,90	-0,04	41,21	-0,03
PP10	0,00	0,99	-20,06	0,62
PP11	0,35	0,42	8,02	0,23

Table 4: Linear regression between maximum extension torque and ball speed for each participant.
P-value (those significant are underlined), coefficient, intercept, and the Pearson's correlation is displayed.

Participant	p-value	Coefficient	Intercept	Correlation
PP01	0,05	0,93	-32,96	0,41
PP02	0,80	0,08	41,08	0,06
PP03	0,00	0,79	-31,16	0,93
PP04	0,19	0,39	4,08	0,28
PP05	0,00	0,60	-4,34	0,64
PP06	0,16	0,68	-6,82	0,32
PP07	0,37	0,20	28,40	0,20
PP08	0,09	0,57	0,45	0,37
PP09	0,59	0,22	18,41	0,12
PP10	0,00	1,00	-18,68	0,67
PP11	0,07	1,02	-29,12	0,42

Table 5: Panel fixed effects ordinary least square analysis on all performed pitches, considering which pitches belonged to which participant, between two parameters. Showing p-value (those significant are underlined), coefficient, intercept and r^2

Dependent	Independent	p-value	Coefficient	Intercept	r^2
Valgus torque	**Extension**	0,00	0,63	12,73	0,31
Valgus torque	**Ball speed**	0,00	0,66	-11,30	0,15
Extension torque	**Ball speed**	0,00	0,64	-7,10	0,17

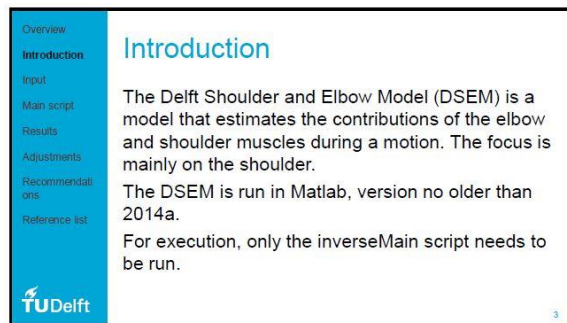## Appendix C – Delft shoulder and elbow model (DSEM)

The following PowerPoint slides provide information on the structure and content of the Delft Shoulder and Elbow Model and the addition of the ulnar collateral ligament.
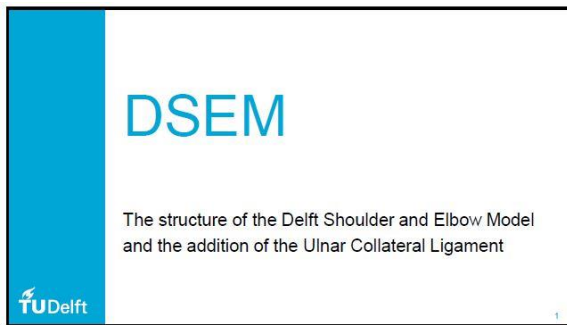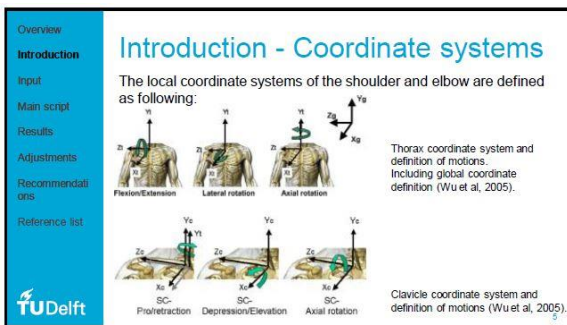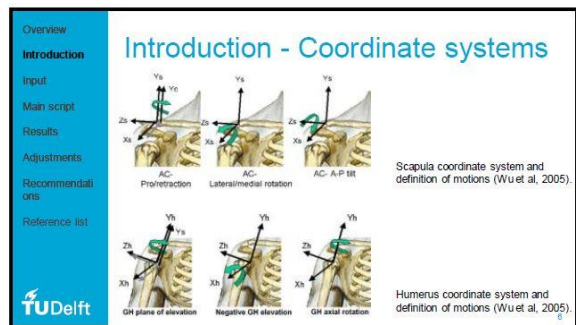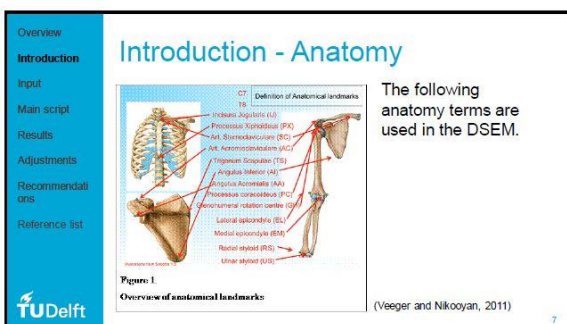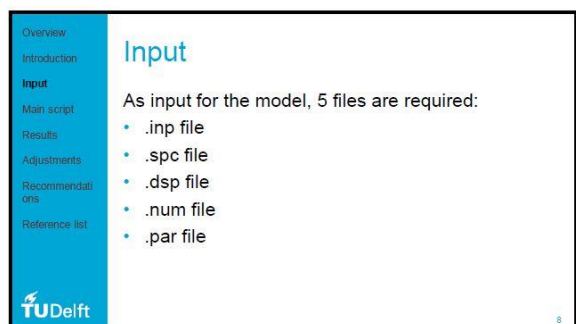

1
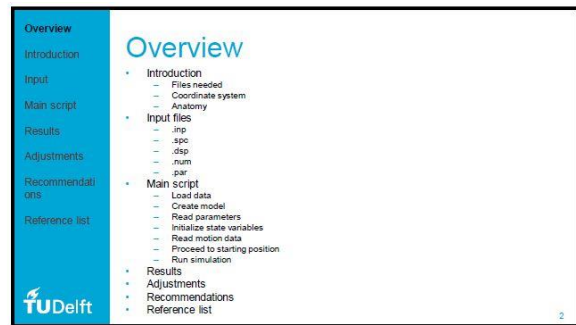
2

3

4

5

6

7

8

Slide 9

Overview
Introduction
Input
Main script
Results
Adjustments
Recommendations
Reference list

Input - .inp

The .inp file is an input file that contains the evaluated motion in joint rotations (degrees).
The rows are the time samples.
The columns represent different motions (see next slide).

Tip: If desired, adjust in Notepad++.

TUDelft

9

Slide 10

Overview
Introduction
Input
Main script
Results
Adjustments
Recommendations
Reference list

Input - .inp

*wrt = with respect to

Columns	Data	Description
1-3	TH	Rotation trunk wrt* global coordinate system (degrees)
4-6	IJ	Position IJ wrt global coordinate system
7-9	SC	Rotation clavicle wrt thorax (degrees)
10-12	AC	Rotation scapula wrt thorax (degrees)
13-15	GH	Rotation GH joint wrt thorax (degrees)
16	ELx	Flexion/extension forearm wrt humerus (degrees)
17	PSy	Pro/supination wrt the ulna (degrees)
18-20	PO	Rotations of the wrist wrt the radius (degrees)
21-23	HF	External forces exerted by the hand wrt global coordinate system (N)
24-26	UM	External moments exerted by the hand wrt global coordinate system (Nm)

TUDelft

10

Slide 11

Overview
Introduction
Input
Main script
Results
Adjustments
Recommendations
Reference list

Input - .inp: 3D Upper Extremity model

If desired, within the 3D Upper Extremity Inverse Dynamics Python model, there is a module that calculates all the joint rotations, using Euler rotations, and creates an .inp file that could be used as an input for the DSEM.

This way, position data, from multiple measuring devices like opto-track & IMU, can be easily transferred to an input file for the DSEM.

TUDelft

11

Slide 12

Overview
Introduction
Input
Main script
Results
Adjustments
Recommendations
Reference list

Input - .spc

The .spc file specifies the bone and joint model.
First, the segment, joint and body marks are defined. Then the muscle crossing joints, force and stress definitions are given.

TUDelft

12

Slide 13

Overview
Introduction
Input
Main script
Results
Adjustments
Recommendations
Reference list

Input - .spc: Abbreviations

mnodeDef = multinode definition.
EINr = element number for each mnodeDef.

Or = orientation nodes, expressed in EINr.
Pos = position node, could consists of insertion point and origin point, expressed in EINr.
Nodenr = each node gets a specific nr.

TUDelft

13

Slide 14

Overview
Introduction
Input
Main script
Results
Adjustments
Recommendations
Reference list

Input - .spc: Segment definition

Segment nr	EINr	Bony segment
1	22	Thorax
2	23	Clavicle
3	24	Scapula
4	25	Humerus
5	26	Ulna
6	27	Radius
7	28	Hand

TUDelft

14

Slide 15

Overview
Introduction
Input
Main script
Results
Adjustments
Recommendations
Reference list

Input - .spc: Joint definition

Joint nr	# DoF	Node Nr	Pos	Or	Position	Joint name
1	3 DoF	32	22	23	04	Thorax
2	3 DoF	33	23	24	07	Clavicle
3	6 DoF*	34, 35, 36	24	25	04	Scapula
4	1 DoF	37	25	26	13	Humerus
5	1 DoF	38	26	27	16	Ulna
6	1 DoF	39	27	28	19	Radius
7	GLD*	40, 41	29	30	-	Hand

* For exceptions, see the Matlab script for explanation.

TUDelft

15

Slide 16

Overview
Introduction
Input
Main script
Results
Adjustments
Recommendations
Reference list

Input - .spc: Bony landmark

Landmark nr	Element nr	Position	Landmark name
1	22	31	Incisura-jugularis (IJ)
2	22	44	Sternoclavicular (SC)
3	24	45	Acromioclavicular (AC)
4	24	46	Angulus-acromialis (AA)
5	24	47	Trigonum-spinae (TS)
6	24	48	Angulus-inferior (AI)
7	25	49	Epicondyle-medial (EM)
8	25	50	Epicondyle-lateral (EL)
9	26	51	Olecranon (OL)
10	26	52	Ulna-styloid (SU)
11	27	53	Radial-styloid (SR)

TUDelft

16

Slide 17

Overview
Introduction
Input
Main script
Results
Adjustments
Recommendations
Reference list

Input - .dsp

The .dsp file is a parameter file containing the morphology information.

For now: l1091fd is used (meaning: Leiden Oct 1991, forward dynamics). Another version is once made specifically for inverse dynamics, but that version isn't working, and the forward dynamics function works fine (even though inverse dynamics is applied).

TUDelft

17

Slide 18

Overview
Introduction
Input
Main script
Results
Adjustments
Recommendations
Reference list

Input - .dsp

Elements within the .dsp file:

- Hinge joints
- Multinode bodies
- Joint positions
- Bony landmarks
- Ligaments
- Wrapping objects
- Muscles (as a truss or as a curve)
- Input generalized coordinates
- Inertial properties

TUDelft

18

Slide 19

Overview
Introduction
Input
Main script
Results
Adjustments
Recommendations
Reference list

Input - .dsp: Restriction definition

There are three ways (among others) to define motion restrictions:

DYNE: A dynamic input where the moments are taken on by the muscles.

RLSE: If off (0) a truss is rigid, if on (1) a truss is released and flexible.

INPUTE: A dynamic input where the moments are not taken on by the muscles.

TUDelft

19

Slide 20

Overview
Introduction
Input
Main script
Results
Adjustments
Recommendations
Reference list

Input - .dsp: Adding the UCL

The UCL is added as a ligament truss (passive element) at element nr 44 (the rest is counted through). Origin at the humerus (segment 25) and insertion at the ulna (segment 26).

The position data are determined as the mean of 3 measurements (dsem50_addUCL/UCL cadaver data Veeger).

No RLSE is added at this ligament since the ligament is modelled as infinitely stiff.

TUDelft

20

Slide 21

Overview
Introduction
Input
Main script
Results
Adjustments
Recommendations
Reference list

Input - .dsp: Adding the UCL

A motion at the elbow in the varus/valgus (Z) direction is allowed by opening up a degree of freedom in this direction at the 'input generalized coordinates' section.

Script: a RLSE is turned on (1) at position 15 (z-direction at the elbow) to allow motion freedom in this direction.

TUDelft

21

Slide 22

Overview
Introduction
Input
Main script
Results
Adjustments
Recommendations
Reference list

Input - .num

The .num file contains information on the muscle and ligament specifications, like first and last truss (or curve) element and the origin and insertion points.

For the addition of the UCL to the DSEM, the ligament is defined in the .num file as ligament 6.

TUDelft

22

Slide 23

Overview
Introduction
Input
Main script
Results
Adjustments
Recommendations
Reference list

Input - .num: Ligament definition

Ligament nr	1st truss	Last truss	Origin	Insertion	Ligament name
1	31	31	23	24	Lig. Conoid
2	32	32	23	24	Lig. Trapezoid
3	33	35	22	23	Lig. Costo-clavicular
4	36	37	22	23	Lig. Sterno-clavicular
5	38	41	24	25	Lig. Gleno-humeral
6	44	44	25	26	Lig. Ulnar-collateral

The sixth ligament is added to include the UCL within the DSEM.

TUDelft

23

Slide 24

Overview
Introduction
Input
Main script
Results
Adjustments
Recommendations
Reference list

Input - .num: Muscle definition

31 muscles of the shoulder and elbow are defined.

Muscle nr, first truss/curve element, last truss/curve element, origin, insertion and muscle names are specified.

TUDelft

24

Slide 25

Overview
Introduction
Input
Main script
Results
Adjustments
Recommendations
Reference list

Input - .par

The .par file contains the 7 filter parameters.

TUDelft

25

Slide 26

Overview
Introduction
Input
Main script
Results
Adjustments
Recommendations
Reference list

Structure of main script

Only the main script, inverseMain.m, should be run to execute the model. This script consists of the following sections:
- Load data
- Create model
- Read parameters
- Initialize state variables
- Read motion data
- Proceed to starting position
- Run simulation

TUDelft

26

Slide 27

Overview
Introduction
Input
Main script
Results
Adjustments
Recommendations
Reference list

Main - Load data

Define the desired .dsp file, .inp file, and .par file. The name of the .dsp file will be used to read the .num and .spc file, so make sure that these three files are saved with the same name.

TUDelft

27

Slide 28

Overview
Introduction
Input
Main script
Results
Adjustments
Recommendations
Reference list

Main - Create model

A model is created, in which all the information will be saved. Define:
- Non-dynamic ('stat') or dynamic ('**dyn**')*
- Print debug information (true/**false**)
- Show calculation progress (**true**/false)
- Print low-level data in each function (true/**false**)

* Default is in bold.

TUDelft

28

Slide 29

Overview
Introduction
Input
Main script
Results
Adjustments
Recommendations
Reference list

Main - Read parameters

The name of the .dsp file at the 'load data' section, will be used to read the .spc and .num files using the same name.

All information from these three files is read and saved in the model.

Printed output: Nr of bony landmarks (n=7) including their element nr and name.

TUDelft

29

Slide 30

Overview
Introduction
Input
Main script
Results
Adjustments
Recommendations
Reference list

Main – Initialize state variables

At the initialization of the state variables, two constraints are defined which influence the shoulder motion:

- Define if motion contain retroflexion. If true, a different deltoid moment arm calculation is performed (new AC and TS defined) and new total degrees of freedoms (default=false).
- Define is fraction file should be provided (this isn't functioning yet, default=false).

TUDelft

30

Slide 31

Overview
Introduction
Input
Main script
Results
Adjustments
Recommendations
Reference list

Main - Read motion data

Motion data from the .inp and .par file are read. Define for the reading of motion:

- First frame for analysis
- Last frame for analysis (0=use all frames)
- *Gap*, step size (1=use each frame, 2=use every other frame, etc.)
- *BeginSteps*, number of steps until the first position

TUDelft

31

Slide 32

Overview
Introduction
Input
Main script
Results
Adjustments
Recommendations
Reference list

Main - Proceed to starting position

Move to starting position to initialize the simulation.

TUDelft

32

Slide 33

Overview
Introduction
Input
Main script
Results
Adjustments
Recommendations
Reference list

Main - Run simulations

Run the simulation to calculate the muscle forces and moments, using the runSimulation.m script.

Define the cost function (now set to 3).

Use the information gained from initializing the state variable, from the process motion and from the start position.

TUDelft

33

Slide 34

Overview
Introduction
Input
Main script
Results
Adjustments
Recommendations
Reference list

Main - Run simulations: Script

In the runSimulation.m script, define at the lines 116:135 which degrees of freedom (segments) should be included in the simulation, 0 means don't include, 1 means include.

To only evaluate the elbow, set only the Hux (flexion/extension) and URy (pro/supination) to 1.

TUDelft

34

Slide 35

Overview
Introduction
Input
Main script
Results
Adjustments
Recommendations
Reference list

Results

The model provides 5 different output results:
- Bone results
- Power
- Muscle force
- Release force
- Netto moment (of the muscles)

TUDelft

35

Slide 36

Overview
Introduction
Input
Main structure
Results
Adjustments
Recommendations
Reference list

Adjustments - UCL addition

Up to now, I only added the UCL as an extra ligament in the model at the .dsp, .spc and .num files.

I opened up a degree of freedom in the direction of varus/valgus in the .dsp file (end of the script).

The motion in the varus/valgus direction is not included in the .inp file, which could be up to discussion if needed (see slide 38).

TUDelft

36

Slide 37

Overview
Introduction
Input
Main structure
Results
Adjustments
Recommendations
Reference list

Adjustments - to get it working

Some additions are made to be able to run the simulation (already implemented in the files of the dsem50_inputChange folder for the evaluation of the baseball pitch and the elbow).

Script	Lines	What?
InverseMain	26-34	Define the desired input files
kernSOLVER	55-78	Comment lines 55-62, uncomment lines 67-78
runSimulation	116-135	Choose which motions to optimize
processMotion	211-216	Comment lines 211-213, uncomment 214-216
InverseMain	120	Choose the correct start and end frame and stepsize according to your input files

TUDelft

37

Slide 38

Overview
Introduction
Input
Main structure
Results
Adjustments
Recommendations
Reference list

Recommendations UCL addition

The .inp file doesn't contain the motion in the varus/valgus direction. Add this and add this also in the 'read motion data'/readAndProcessMotionData.m/processMotion.m and other scripts. The varus/valgus angles will be relatively small compared to the flexion/extension angles, and almost impossible to measure with marker analysis. More advanced techniques, like ultrasound, could help provide more information on these angles during the baseball pitch.

TUDelft

38

Recommendations UCL addition

Overview
Introduction
Input
Main structure
Results
Adjustments
Recommendations
Reference list

The DSEM now only calculates the muscle forces and muscle moments (defined at runSimulation.m lines 487-497, only nodes of muscles are considered). Expand this in an equal matter to also calculate ligament forces and moments.

I made a beginning on how this could be calculated and what should be done. However, the current function is not yet working as desired. In the next slide I provide the current versions of the adjusted scripts and the changes I made (save in dsem50_addUCL folder).

TUDelft

39

Recommendations UCL addition

Overview
Introduction
Input
Main structure
Results
Adjustments
Recommendations
Reference list

Script	Lines	What?
kernMinFFSQPB	Begin & 354-365	Add ligament part to calculate lower and upper bound
kernFOREL	99-103	Initialize the ligament force
runSimulation	461	Add BUL
runSimulation	500-510	Add ligament calculations
runSimulation	90	Add ligament initiation
Model	427	Add the ligament Force and ReleaseForce as outcomes of the model
processUSRfiles	120	Initialize the elmntligUCL that will later be defined in elemPrepSPC
elemPrepSPC	111	Add to nummatcom a parameter liglen which is the amount of mnodes in the ligament. Could be neater but this worked for now.

TUDelft

40

Recommendations UCL addition

Overview
Introduction
Input
Main structure
Results
Adjustments
Recommendations
Reference list

Dsem50_addUCL folder contains information on the addition of the UCL:
- Matlab scripts: scripts where a start is made on the recommendations of slide 40.
- UCL cadaver data Veeger: cadaver data based on which the position data of the UCL is determined

In the overall DSEM folder useful documents to understand the structure of the DSEM and the addition of the UCL are added in the folder 'Documents'.

TUDelft

41

Recommendations UCL addition

Overview
Introduction
Input
Main structure
Results
Adjustments
Recommendations
Reference list

Data management plan DSEM:

TUDelft

42

Reference list

Overview
Introduction
Input
Main structure
Results
Adjustments
Recommendations
Reference list

- Veeger, H. E. J., & Nikooyan, A. A. (2011, August 2). A standardized protocol for motion recordings of the shoulder. TU Delft. http://homepage.tudelft.nl/g6u61/shoulder_cookbook/overview_3.htm
- Wu, G., Van Der Helm, F. C. T., Veeger, H. E. J., Makhsous, M., Van Roy, P., Anglin, C., Nagels, J., Karduna, A. R., McQuade, K., Wang, X., Werner, F. W., & Buchholz, B. (2005). ISB recommendation on definitions of joint coordinate systems of various joints for the reporting of human joint motion - Part II: Shoulder, elbow, wrist and hand. *Journal of Biomechanics*, *38*(5), 981–992. https://doi.org/10.1016/j.jbiomech.2004.05.042

TUDelft

43

Appendix D – Data management plan

The data management plan provides insight into how all the relevant files of this research are structured in two folders. Figure 1 displays the folder set-up of the 3D inverse dynamics Python model. Figure 2 and 3 shows how within the 3D inverse dynamics Python model the data is treated and saved between each step of the calculations. For more detail on the setup of the model, see Appendix A. Figure 4 displays the folder set-up of the Delft Shoulder and Elbow Model (DSEM), where the 'dsem50_inputChange' is the main folder.
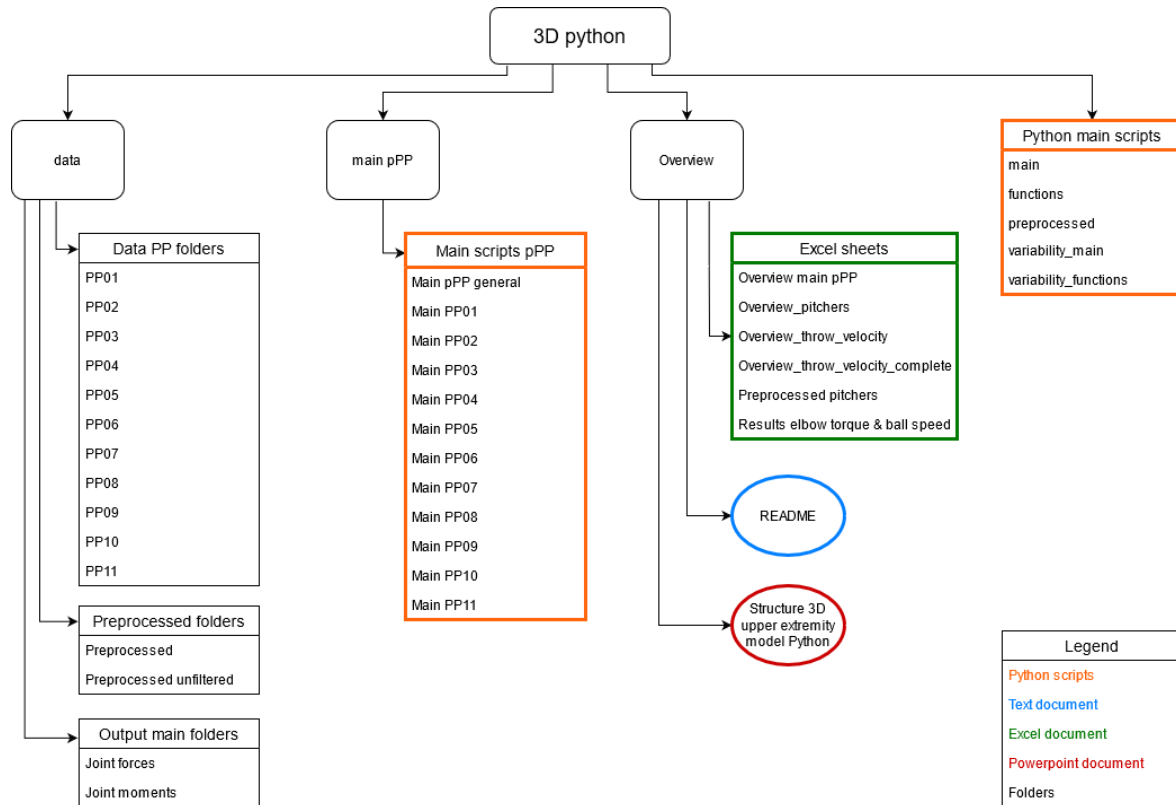
Figure 1: Folder structure containing the files needed for or providing information on the 3D inverse dynamics python model.
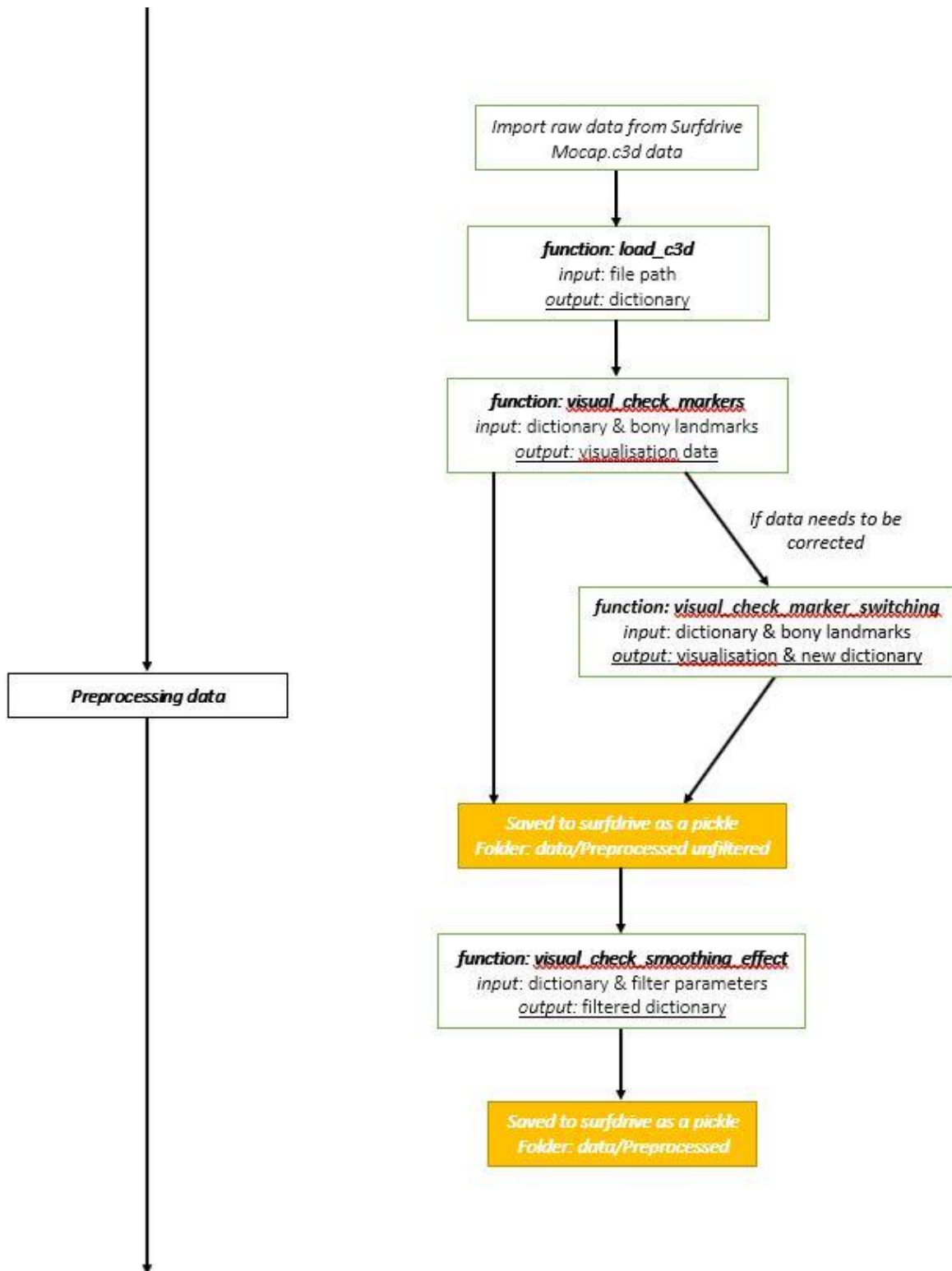
Figure 2: Data management of the 3D inverse dynamics python model, part 1: from the raw Vicon data to the preprocessed position data.
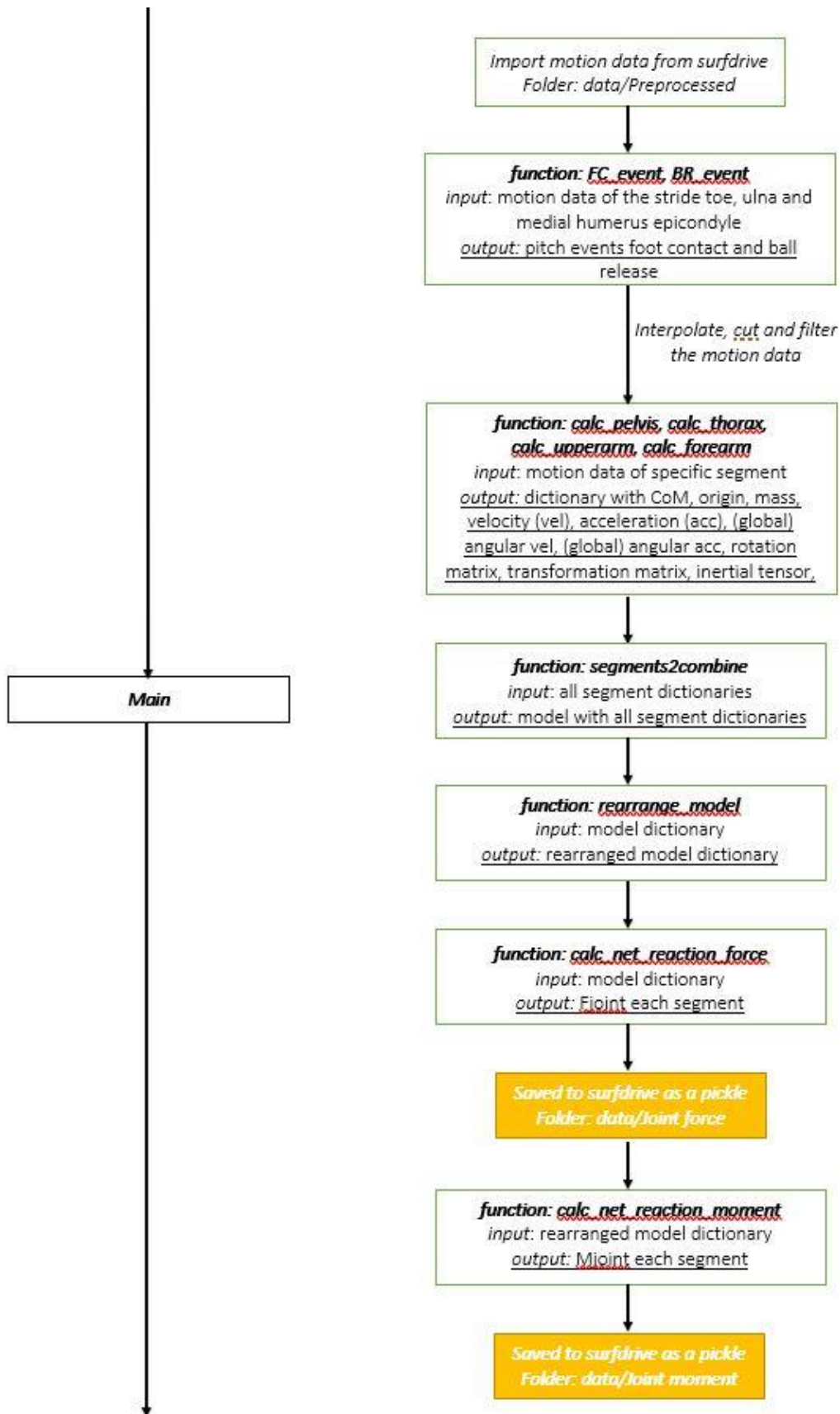
.

Figure 3: Data management of the 3D inverse dynamics python model, part 2: from the preprocessed position data to the joint forces and joint torques.
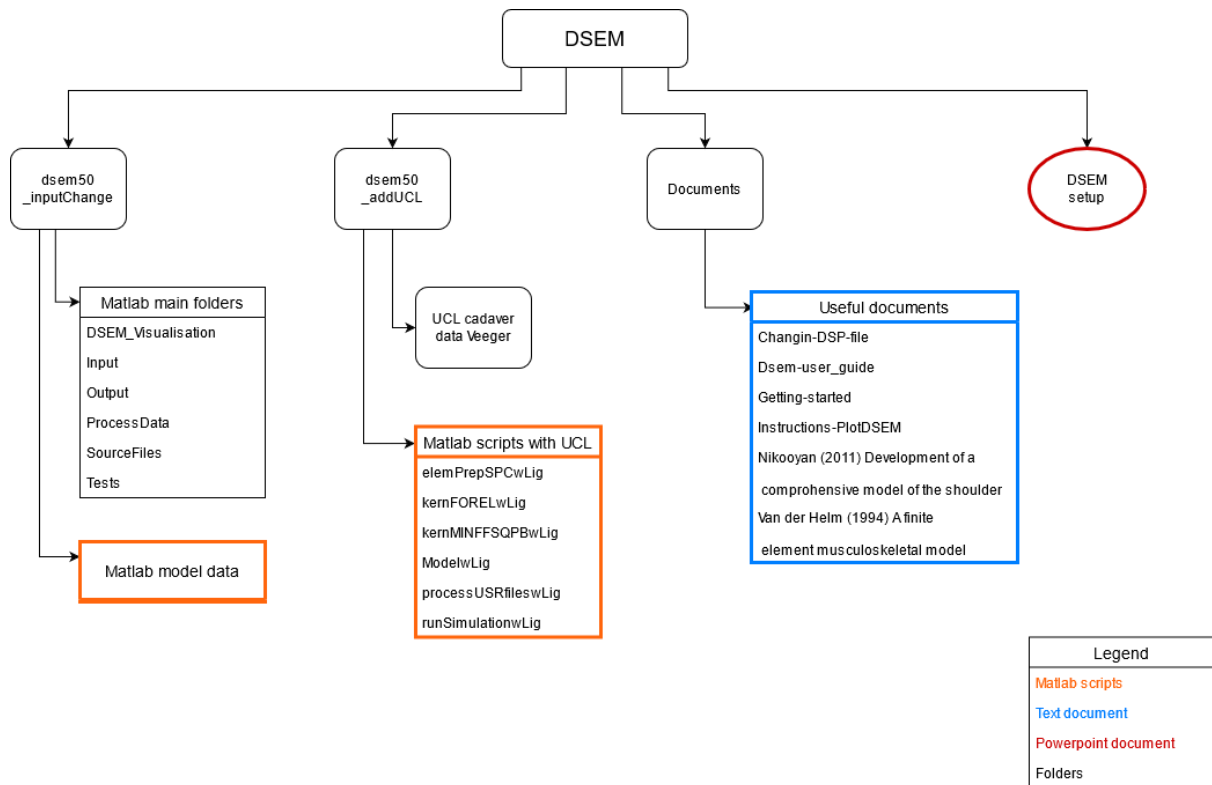
Figure 4: Folder structure containing the files needed for or providing information on the DSEM.